

AD-A163 821

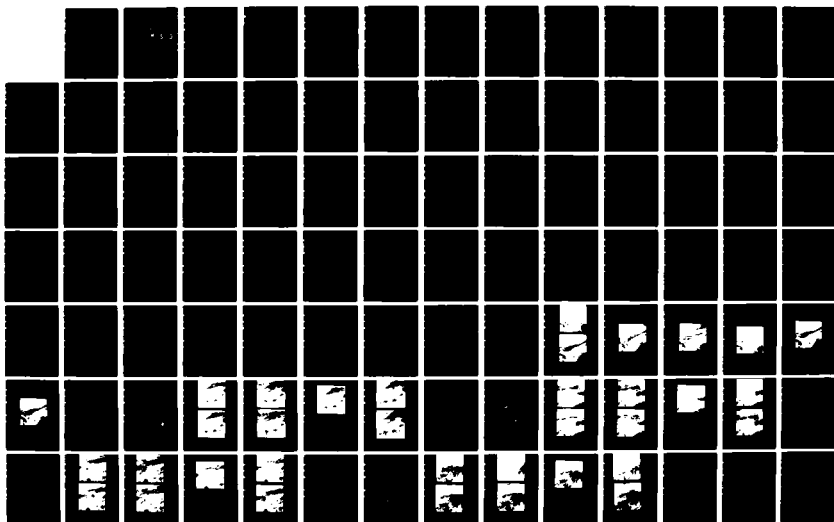
SATELLITE CLOUD AND PRECIPITATION ANALYSIS USING A
MINICOMPUTER(U) NAVAL POSTGRADUATE SCHOOL MONTEREY CA
C H WASH ET AL NOV 85 NPS-63-85-003

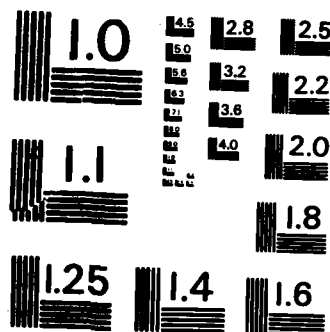
1/1

UNCLASSIFIED

F/G 4/2

NL





MICROCOPY RESOLUTION TEST CHART
NATIONAL BUREAU OF STANDARDS-1963-A

2

NPS-63-85-003

AD-A163 821

NAVAL POSTGRADUATE SCHOOL

Monterey, California



DTIC
ELECTE
FEB 06 1986
S D
D

Satellite Cloud and Precipitation Analysis
Using a Minicomputer

by

Carlyle H. Wash

Laura A. Spray

Lang C. Chou

November 1985

Technical Report Period: October 1983 - October 1985

DTIC FILE COPY

Approved for Public Release; Distribution Unlimited.

Prepared for: Naval Environmental Prediction Research Facility
Monterey, CA 93943

86 2 6 112

Naval Postgraduate School
Monterey, California

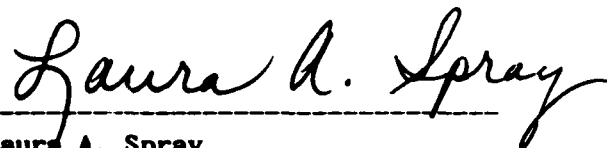
Rear Admiral Robert H. Shumaker
Superintendent

David A. Schrady
Provost

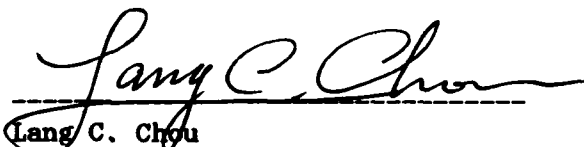
This report was prepared by:



Carlyle H. Wash
Associate Professor of Meteorology
Department of Meteorology
(408) 646-2295



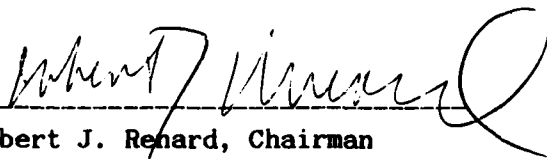
Laura A. Spray
Meteorologist
Department of Meteorology
(408) 646-3110



Lang C. Chou
Meteorologist
Department of Meteorology
(408) 646-3110

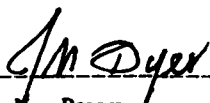
Publication of the report does not constitute approval of the sponsor for the findings or conclusions. It is published for information and for the exchange and stimulation of ideas.

Reviewed by:



Robert J. Renard, Chairman
Department of Meteorology

Released by:



John N. Dyer
Dean of Science and Engineering

Date

SECURITY CLASSIFICATION OF THIS PAGE (When Data Entered)

DD FORM 1473
1 JAN 73

UNCLASSIFIED

SECURITY CLASSIFICATION OF THIS PAGE (When Data Entered)

UNCLASSIFIED

SECURITY CLASSIFICATION OF THIS PAGE(When Data Entered)

for an approximately 1600 x 1600 n mi area over the eastern United States and western North Atlantic Ocean are used in evaluating the model's performance. Each satellite-derived cloud and precipitation analysis is evaluated subjectively, using conventional synoptic data, radar measurements and manual nephanalysis for verification, and objectively, using surface synoptic observations for verification. Successful estimates of cloud amount for overcast and clear skies were obtained; however, broken and scattered conditions were underestimated. The majority of stratiform cloud types and multi-layered clouds were analyzed correctly by the model. Classification errors occurred with cumuliform clouds and thin cirrus. Reasonable precipitation intensity and cloud-top temperature/height analyses were produced by the Naval Postgraduate School model.

UNCLASSIFIED

SECURITY CLASSIFICATION OF THIS PAGE(When Data Entered)

ABSTRACT

A satellite-derived cloud and precipitation analysis program has been developed for an interactive mini-computer system. The program utilizes geostationary infrared and visual data with operational upper air and surface temperature analyses to specify cloud type, cloud amount, cloud-top temperature, cloud-top height and estimated precipitation intensity.

Five cases of GOES-East data (2 x 2 n mi visual and 2 x 4 n mi infrared) for an approximately 1600 x 1600 n mi area over the eastern United States and western North Atlantic Ocean are used in evaluating the model's performance. Each satellite-derived, cloud and precipitation analysis is evaluated subjectively, using conventional synoptic data, radar measurements and manual nephanalysis for verification, and objectively, using surface synoptic observations for verification.

Successful estimates of cloud amount for overcast and clear skies were obtained; however, broken and scattered conditions were underestimated. The majority of stratiform cloud types and multi-layered clouds were analyzed correctly by the model. Classification errors occurred with cumuliform clouds and thin cirrus. Reasonable precipitation intensity and cloud-top temperature/height analyses were produced by the NPS model.

*Keywords: GOES (Geostationary
Operational Environmental Satellite)*



Accession For	
NTIS	CRA&I <input checked="" type="checkbox"/>
DTIC	TAB <input type="checkbox"/>
Unannounced <input type="checkbox"/>	
Justification	
By	
Distribution/	
Availability Codes	
Dist	Avail and/or Special
A-1	

ACKNOWLEDGEMENT

This work was funded by the Naval Environmental Prediction Research Facility, Monterey, CA under Program Element 62759N, Project WF59-553, "GOES Data Analysis for Weather Analysis and Forecasting."

TABLE OF CONTENTS

List of Figures.....	4
List of Tables.....	7
1. Introduction.....	8
2. NPS Cloud and Precipitation Analysis Model.....	10
3. Evaluation Plan.....	16
4. Evaluation Results.....	18
5. Statistical Evaluation Plan.....	38
6. Statistical Evaluation Results.....	43
7. Summary and Conclusions.....	49
List of References.....	52
Appendix A.....	53
Appendix B.....	57
Initial Distribution List.....	91

LIST OF FIGURES

- Figure 1a. Two-dimensional cloud typing graph using GOES IR and VIS satellite digital data.....57
- Figure 1b. Two-dimensional precipitation estimate graph using GOES IR and VIS satellite digital data.....57
- Figure 2. Geographic location of study region.....58
- Figure 3. GOES VIS imagery for 02 AUG 83.....59
- Figure 4. GOES IR imagery for 02 AUG 83.....59
- Figure 5A. Cloud amount analysis for 02 AUG 83.....60
- Four grayshades are used to distinguish between cloud amounts: 100% cloud cover (OVC), lightest grayshade; 75% cloud cover (BRO), medium grayshade; 50% cloud cover (SCA), darkest visible grayshade; 25% cloud cover (CLR-SCA), darkest grayshade (unable to distinguish on photo).
- Figure 5B. Cloud type analysis for 02 AUG 83.....61
- Eight grayshades are used to illustrate eight different cloud types. Cloud types in decreasing order of grayshade brightness are as follows: cumulonimbus (Cb), lightest grayshade; nimbostratus (Ns); cumulus congestus (Cu Cong); cumulus (Cu); stratocumulus (Sc); stratus (St); altostratus (As); cirrus (Ci), darkest grayshade.
- Figure 5C. Precipitation intensity analysis for 02 AUG 83.....62
- Three grayshades are used to distinguish between precipitation intensities: heavy (3), lightest grayshade; moderate (2), medium grayshade; light (1), darkest grayshade.
- Figure 5D. Cloud-top temperature analysis for 02 AUG 83.....63
- Nine grayshades are used to illustrate 10 K intervals of cloud-top temperatures. Cloud-top temperature 10 K intervals in order of decreasing grayshade brightness are as follows: 210-219 K, lightest grayshade; 220-229 K; 230-239 K; 240-249 K; 250-259 K; 260-269 K; 270-279 K; 280-289 K, darkest visible grayshade; 290-300 K, surface values

Figure 5E.	Cloud-top height analysis for 02 AUG 83.....	64
<p>Nine grayshades are used to illustrate 100 mb cloud-top height intervals. Cloud-top height 100 mb intervals in order of decreasing grayshade brightness are as follows: 100-199 mb, lightest grayshade; 200-299 mb; 300-399 mb; 400-499 mb; 500-599 mb; 600-699 mb; 700-799 mb, darkest visible grayshade; 800-899 mb (unable to distinguish on photo); 900-1000 mb, darkest grayshade (unable to distinguish on photo).</p>		
Figure 6.	Surface observation and ARS verification chart for 02 AUG 83.....	65
Figure 7.	Manual satellite analysis verification chart for 02 AUG 83. Standard abbreviations are used to identify cloud types. Darkened areas represent thick, multiple cloud layers.....	66
Figure 8.	GOES VIS imagery for 11 AUG 83.....	67
Figure 9.	GOES IR imagery for 11 AUG 83.....	67
Figure 10A.	Same as Fig. 5A except for 11 AUG 83.....	68
Figure 10B.	Same as Fig. 5B except for 11 AUG 83.....	68
Figure 10C.	Same as Fig. 5C except for 11 AUG 83.....	69
Figure 10D.	Same as Fig. 5D except for 11 AUG 83.....	70
Figure 10E.	Same as Fig. 5E except for 11 AUG 83.....	70
Figure 11.	Surface observation and ARS verification chart for 11 AUG 83.....	71
Figure 12.	Manual satellite analysis verification chart for 11 AUG 83. Standard abbreviations are used to identify cloud types. Darkened areas represent thick, multiple cloud layers.....	72
Figure 13.	GOES VIS imagery for 23 AUG 83.....	73
Figure 14.	GOES IR imagery for 23 AUG 83.....	73
Figure 15A.	Same as Fig. 5A except for 23 AUG 83.....	74
Figure 15B.	Same as Fig. 3D except for 23 AUG 83.....	74
Figure 15C.	Same as Fig. 3E except for 23 AUG 83.....	75
Figure 15D.	Same as Fig. 3F except for 23 AUG 83.....	76
Figure 15E.	Same as Fig. 3G except for 23 AUG 83.....	76

Figure 16.	Surface observation and ARS verification chart for 23 AUG 83.....	77
Figure 17.	Manual satellite analysis verification chart for 23 AUG 83. Standard abbreviations are used to identify cloud types. The abbreviations MLMC and ML Cld are used for multi-layered middle cloud and multi-layered cloud, respectively. Darkened areas represent thick, multiple cloud layers.....	78
Figure 18.	GOES VIS imagery for 31 AUG 83.....	79
Figure 19.	GOES IR imagery for 31 AUG 83.....	79
Figure 20A.	Same as Fig. 5A except for 31 AUG 83.....	80
Figure 20B.	Same as Fig. 5B except for 31 AUG 83.....	80
Figure 20C.	Same as Fig. 5C except for 31 AUG 83.....	81
Figure 20D.	Same as Fig. 5D except for 31 AUG 83.....	82
Figure 20E.	Same as Fig. 5E except for 31 AUG 83.....	82
Figure 21.	Surface observation and ARS verification chart for 31 AUG 83.....	83
Figure 22.	Manual satellite analysis verification chart for 31 AUG 83. Standard abbreviations are used to identify cloud types. Darkened areas represent thick, multiple cloud layers.....	84
Figure 23.	GOES VIS imagery for 02 SEP 83.....	85
Figure 24.	GOES IR imagery for 02 SEP 83.....	85
Figure 25A.	Same as Fig. 5A except for 02 SEP 83.....	86
Figure 25B.	Same as Fig. 5B except for 02 SEP 83.....	86
Figure 25C.	Same as Fig. 5C except for 02 SEP 83.....	87
Figure 25D.	Same as Fig. 5D except for 02 SEP 83.....	88
Figure 25E.	Same as Fig. 5E except for 02 SEP 83.....	88
Figure 26.	Surface observation and ARS verification chart for 02 SEP 83.....	89
Figure 27.	Manual satellite analysis verification chart for 02 SEP 83. Standard abbreviations are used to identify cloud types. Darkened areas represent thick, multiple cloud layers.....	90

LIST OF TABLES

Table 1. Cloud/precipitation grayshade categories in order of decreasing brightness.....	53
Table 2. Statistical evaluation results of single cloud types..	54
Table 3. Statistical evaluation results of multi-layered clouds.....	55
Table 4. Statistical evaluation results of precipitation occurrence.....	56

I. Introduction

Satellite imagery has become an important tool for today's meteorologist. Significant mesoscale and subsynoptic scale (10-1000 km) meteorological phenomena, not readily discernible through either synoptic or airway surface observations or 12-hourly upper-air reports, often can be determined from an interpretation of satellite imagery. Interpretation of satellite imagery, however important, is difficult because of the time and skill required and the subjective nature of the analysis. Another difficulty is the limited ability to use satellite data in digital, rather than quantitative, form. Because of these constraints, operational meteorologists often rely on the imagery as a source of information for determining only the gross synoptic-scale features, such as frontal placement, ridge axes and surface pressure centers. The true potential of digital satellite data is often not fully utilized by the operational meteorologist.

The first objective of this technical report is to describe an automated cloud and precipitation intensity model. Specifically, this model was designed to produce, in real-time (five minutes), analyses of important cloud and weather features, such as cloud amount, cloud type, cloud-top temperature, cloud-top height and precipitation intensity. These analyses are possible through interactive minicomputer processing of digital satellite data, a capability soon to be available to the operational meteorologist. Analyses are based on digital satellite data from the Geostationary Operational Environmental Satellite (GOES) System using the visual and infrared channels,

which have a spatial resolution of 0.5 to 4.0 n mi respectively, and are available every thirty minutes.

A second objective of this report is to record the evaluation of these cloud and precipitation intensity analyses utilizing the Satellite Processing and Display System (SPADS) at the Naval Environmental Prediction Research Facility (NEPRF) in Monterey, California and the VAX/COMTAL system of the Computer Science Laboratory at the Naval Postgraduate School (NPS). Systematic evaluation of significant meteorological features is conducted with GOES-East imagery for regions in the southeastern United States. Verification data consists of subjective manual analyses of the imagery, conventional surface observations and the National Weather Service Automated Radar Summary (ARS) chart (National Oceanic and Atmospheric Administration, U.S. Department of Commerce, 1979). A statistical evaluation of the model's cloud type and precipitation analyses using ground truth data concludes the report.

II. NPS Cloud and Precipitation Analysis Model

The Naval Postgraduate School (NPS) automated cloud and precipitation model produces real-time analyses of important cloud and precipitation parameters including cloud amount, cloud type, cloud-top temperature, cloud-top height and precipitation intensity. The automated cloud model was developed by Nelson, (1982) who utilized Harris and Barrett's (1978) cloud amount estimate techniques, Liljas' (1982) cloud and precipitation intensity threshold method and Reynolds and Vonder Haar's (1977) bispectral cloud-top temperature scheme. The model's performance was first evaluated by Moren (1984). Wyse (1984) studied the merger of conventional surface data with the satellite data to produce final analyses dependent upon both satellite data and surface observations. This report describes the model and its performance after revisions were made based on Moren's evaluation.

The NPS cloud model uses digital satellite data from the visual and infrared channels from the GOES Visual-Infrared Spin Scan Radiometer (VISSR) and performs a movable window analysis anywhere within the satellite area coverage. The basic configuration of the data is a 1024 x 1024 n mi area (256 x 256 grid array). A 2 x 2 grid (2 x 2 n mi) of visual data corresponds to one repeated (2 x 4 n mi) infrared pixel. The cloud and precipitation output fields are available at each infrared pixel.

The NPS cloud model is composed of three main processors: (1) data input, (2) basic satellite and statistical calculations and (3) cloud and precipitation computations. Satellite

calculations include conversion of infrared data counts to infrared temperatures using the the GOES sensor conversion table (Corbell et al., 1978) and visual data counts to albedos using the brightness normalization scheme of Muench and Keegan (1979), to correct for sun angle and anisotropy. These infrared temperatures and albedos are used in the model instead of the raw GOES sensor counts. Temperature-pressure soundings are obtained from the Fleet Numerical Oceanography Center (FNOG) for the center point of sixteen subsections of the infrared image.

Further processing of the visual data results in an average brightness and its standard deviation for each 2 x 2 grid array. The average visual brightness value and corresponding infrared temperature, together with brightness standard deviation, are used to produce the cloud and precipitation analyses.

A. Cloud Amount

Cloud amount is determined by comparing the visual albedos with a 0.17 threshold background brightness value which is dependent upon the general visual radiance reflected by the summer land surface. This threshold was arrived at empirically and represents a higher level than in Liljas (1982). Keegan and Niedzielski (1981) determined the average albedo to be approximately 0.13 for a 9 x 9 array of pixels (1.0 n mi resolution) for the 1977-78 autumn/spring/summer over the northeastern United States. Tsonis (1984) defined the cloud/no cloud threshold range to be between 24 and 27 raw GOES sensor counts (corresponding to a 0.12- 0.19 albedo range), depending

upon the surface characteristics. Average cloud amount at each infrared pixel is computed following Harris and Barrett (1978) and Fye (1978):

$$A = 100 (M/N)^2 \quad M = \sum_{i=1, N}^N d_{ij}$$

where A is the average cloud amount
 N is the number of rows/columns (in this case N=2)
 d is a step function, either 1 or 0 depending upon
 whether the individual visual pixel threshold
 exceeds the cloud/no cloud threshold criterion.

In this application cloud amount estimate then takes on the values of 0, 0.25, 0.50, 0.75 or 1.0. Using a larger array of satellite data would allow more variation but would require more computer time.

B. Cloud Type

The bispectral classification uses infrared temperatures, visible albedos, and in some cases visible standard deviation values, to discriminate cloud type. The average visible brightness values and infrared temperatures are used in a series of threshold tests following Liljas (1982) in determining a particular cloud type (Fig. 1a). In the case of discriminating between stratus and cumulus, stratocumulus and cumulus, and altostratus and cumulus congestus, a texture test is conducted with the brightness standard deviation. Harris and Barrett (1978) performed a linear discriminant analysis using standard deviation values and vector dispersion to separate cumuliform and stratiform clouds. If the standard deviation is greater than the threshold value 0.05, then the cloud type is cumuliform due to the variation in albedo values. A standard deviation less than 0.05 results in a stratiform cloud type

classification. A typical brightness standard deviation range for stratiform clouds is between 0.01 and 0.04.

C. Precipitation Intensity

Precipitation estimation follows Liljas' (1982) threshold technique, adopted from the results of Muench and Keegan (1979). The technique relates the cloud type information to precipitation areas. If the resulting cloud type is nimbostratus or cumulonimbus, the precipitation thresholds are activated. Three categories of intensity (light, moderate, heavy) can result depending upon the infrared temperature and visual albedo (Fig. 1b).

D. Cloud-top Temperature/Height

The Reynolds and Vonder Haar (1977) bispectral approach is used for estimating cloud-top temperatures. The bispectral method provides a better analysis of cloud-top temperatures than using only the infrared channel. Situations that show the most improvement are cirrus layers and partially-filled fields of view since the bispectral method includes surface radiance estimates. Cloud amount (already calculated), emissivity and surface radiance are used to compute cloud-top temperatures. A 0.9 emissivity is used for all cloud types except thick clouds such as nimbostratus or cumulonimbus which are assigned an emissivity of 1.0. Although Reynolds and Vonder Haar suggested a 0.55 emissivity for cirrus-type clouds, the cirrus analyzed by the model in this study were thick and an emissivity of 0.9 was used. Objectively classifying thin cirrus (for which the lower

emissivity is appropriate) is still a problem. The surface temperatures are obtained from the Fleet Numerical Oceanography Center (FNOC) soundings and converted to radiance via the Planck function. The following equation calculates the final infrared cloud-top radiance:

$$\text{RADCLD} = (\text{RADMEA} - \text{RADSFC}) / (\text{CLOUDAMT} * \text{EMISSION}) + \text{RADSFC}$$

where RADCLD is the infrared cloud-top radiance
RADMEA is the measured infrared radiance
RADSFC is the surface infrared radiance from a clear area
CLOUDAMT is the cloud amount
EMISSION is the cloud emissivity

The cloud-top temperature results from applying the Inverse Planck function to the cloud-top radiance. Finally, the temperature is equated to a pressure-level height (mb) from the FNOC soundings.

Several modifications were made to the model based on the evaluation results of Moren (1984). The cloud/no cloud threshold was raised from 0.11 to 0.17. Many clear and scattered cumulus areas, which were depicted as overcast using a 0.11 threshold, were analyzed correctly using a 0.17 threshold. The visible threshold, which distinguishes stratus from stratocumulus and cirrus from cumulus congestus, was raised from 0.31 to 0.55 since better cloud type analyses were produced with the greater threshold. The standard deviation used in the texture test to separate cumuliform and stratiform clouds was lowered from 0.25 to 0.05, based on several standard deviation computations for both stratiform and cumuliform clouds. A texture test was applied to differentiate altostratus from cumulus congestus since these clouds have similar infrared temperatures and visible

albedos but have different texture characteristics. The texture test used to distinguish cirrus from altostratus was eliminated; these cloud types can be separated better with a 0.55 visible threshold. The infrared threshold used to differentiate between stratocumulus and cumulus congestus was lowered from 271 K to 264 K since the majority of stratocumulus/cumulus congestus had temperatures below/above 264 K. The precipitation/no precipitation thresholds were modified to produce better analyses. The infrared temperature threshold was lowered from 251 K to 249 K and the visible albedo threshold was raised from 0.31 to 0.55. The plan used to evaluate the current NPS model is described in the following chapter.

III. Evaluation Plan

The verification region is centered over the eastern United States with the center point of the 512 x 512 satellite array located at 35°N 80°W. This geographical location is selected to cover a variety of meteorological phenomena (including coastal, land and ocean cloud features); to maximize the surface and upper-air station verification data network and meteorological observational pilot reports; to facilitate the satellite retrieval by NEPRF; and to illustrate further use of the automated satellite cloud analysis program on the SPADS unit at Naval Eastern Oceanography Center (NEOC) at Norfolk, Virginia.

The digitized GOES sectors from 1500 GMT are analyzed with a center point at 35°N 80°W. The 512 x 512 visual array (2 x 2 n mi) and 256 x 256 infrared array (2 x 4 n mi at sub-satellite point) have an approximate 1600 x 1600 n mi area coverage. Concurrently, FNOC 1200 GMT analysis soundings are obtained. Sixteen grid points, each centered on the sixteen 64 x 64 infrared pixel arrays (128 x 128 visible pixel arrays) are established. Surface and upper-level temperature profiles are extracted for each center point.

The NPS model's performance is evaluated subjectively, using manual analysis of the imagery prepared independently of the computer analysis, and conventional 1500 GMT surface data. The 1200 GMT upper-air observations and 1535 GMT Automated Radar Summary (ARS) chart are also utilized.

A statistical evaluation is performed on each case for cloud type classification and precipitation occurrence. Synoptic land,

ship and hourly airways observations (approximately 75 stations) scattered throughout the geographic study region are used for verification. Each valid surface observation of cloud type and precipitation is compared to the automated analysis. For each case the percentage correct is calculated for each cloud type classification. The percentage correct is obtained from the total number of cloud type agreements between the surface observations and the satellite data in a particular cloud type category, divided by the number of surface stations reporting that cloud type. The surface reports of multi-layered clouds are evaluated differently since no distinction is made between nimbostratus and multi-layered clouds in the NPS cloud-typing routine.

A percentage correct scheme is also used on the precipitation data. Each surface report of precipitation is compared to the satellite's precipitation classification of either rain or no rain. The percentage of agreement between the surface report and satellite data is computed. The same percentage correct method is applied to the no-precipitation case.

Five summer case studies are presented in this report to illustrate the accuracy and utility of the NPS cloud and precipitation analyses. The evaluation dates are 02 AUG 83, 11 AUG 83, 23 AUG 83, 31 AUG 83 and 02 SEP 83.

IV. Evaluation Results

For each of the five cases evaluated, the GOES visual and infrared input data are presented first followed by cloud analysis of amount, type, precipitation intensity, cloud-top temperature and height. The ARS with selected surface observations and a manual satellite analysis are used as verification data for each case. Fig. 2 shows the geographic area of all cases. Geographic outlines are not included on the satellite data to avoid masking the data. An acetate grid is included for reference on these figures.

A. 02 AUGUST 1983

1. SYNOPTIC DESCRIPTION

In the 02 AUG case a 1010 mb low develops near the St. Lawrence river at the peak of the warm sector. The trailing cold front extends across the eastern New England states into New Jersey, Maryland, northern Virginia and northern Tennessee and Arkansas. Cold dry air flowing about a 1024 mb high near Lake Michigan and warm moist air about the Bermuda high produces an active frontal boundary (Figs. 3 and 4).

2. CLOUD AMOUNT

The NPS cloud amount estimates (Fig. 5A) for clear and overcast skies as well as the cloud boundary definition are accurate for this case. This cloud amount analysis shows some significant, interesting cloud patterns in the Great Lakes area, the Gulf coast states, and the frontal band region. Broken (75% cloud cover) and scattered (50% cloud cover) conditions are underestimated by the NPS algorithm. (The scattered-clear

category, 25% cloud cover, is indistinguishable in the photographs after reproduction.) The estimation of cloud amount is directly related to the size of the array used to compute fractional cloud cover. A 2×2 matrix of visible albedos encompassing approximately 4 n mi allows only five fractional cloud amounts (0, 0.25, 0.50, 0.75, 1.0). Using a larger array for computing cloud amount will improve the range of scattered and broken estimates. With the 2×2 array, fields of larger cumulus will be classified as clear or overcast/broken in a random pattern. This estimate is consistent with a cloud cover percentage for small regions. If the user needs a percentage of cloud cover over a larger field of view, a larger array would be appropriate, producing a more continuous distribution of cloud amount percentages.

A good example of the depiction of a broken cloud field is in the cold air mass behind the frontal boundary over the Great Lakes region in Fig. 5A. Consistent with the GOES visual and infrared data, the surface observations (Fig. 6) and manual satellite analysis (Fig. 7), the NPS analysis indicates that clouds are absent over the Great Lakes while broken and overcast cloud bands exist over the adjacent land areas.

The first evaluation of the NPS model, conducted by Moren (1984), depicted the region over Indiana, Illinois, Wisconsin and Michigan as broken and scattered, whereas the surface observations and manual satellite analysis (Fig. 6) indicated scattered and clear conditions. The current NPS analysis agrees with the verification data indicating little or no cloud cover in

this region.

Over the Gulf coast states in the cyclone warm sector the cloud amount analysis is reasonable. The scattered regions ahead of the cold front over southern Alabama and southwestern Georgia as well as the overcast region over northern Florida and scattered-clear region over southern Florida are accurately depicted.

The NPS model produces a fairly accurate cloud amount estimation and distribution analysis of the ENE to WSW broadening frontal band. The verification data suggests broken and overcast skies which agrees with this current analysis. The earlier model had overestimated the cloud amount in this region.

3. CLOUD TYPE

Cloud type classification from the model is presented in Fig. 5B. Three cloud type areas are designated for discussion from this case: the frontal cloud types, the cloud types in the southeast quadrant of the sector and the cloud types in the northeast quadrant.

The frontal cloudiness has an ENE-WSW orientation and extends across the complete analysis region and broadens over the western quadrant. In the eastern portion of the cold front, the automated analysis of nimbostratus/multi-layered clouds are verified by manual satellite analysis as multi-level thick clouds. Over North Carolina and Virginia, the model indicates multi-layered/nimbostratus, altostratus, cirrus, with cumulus congestus to the south. Both the surface observations (Fig. 6) and manual satellite analysis (Fig. 7) indicate multi-layered

middle and high clouds with cumulus build-ups to the south. The earlier NPS model overestimated the amount of nimbostratus/multi-layered cloud in this region. In the western section of the cold front, the automated analysis indicates cumulus congestus, multi-layered/nimbostratus, altostratus, stratocumulus and cumulus cloud types, which agrees with both the surface observations and manual satellite analysis.

In the southeast quadrant, the NPS model depicts a large region of cumulonimbus, nimbostratus/multi-layered clouds and cumulus congestus, with adjacent cirrus to the west. The earlier version indicated altostratus instead of cirrus in this region. This successful cirrus classification results from eliminating the texture test used to separate cirrus and altostratus and using a visible threshold to distinguish cirrus (visible albedo less than 0.55) from altostratus (visible albedo greater than or equal to 0.55).

In the northeast quadrant, the analysis depicts cumulus, stratocumulus and a small area of multi-layered clouds. This pattern develops as cool air north of the front moves southeastward into northeastern United States. This analysis is in agreement with the surface observations (Fig. 6) and manual satellite analysis (Fig. 7). The earlier NPS model incorrectly indicated peripheral stratus/fog along the southern boundary of the cloud mass; the current version gives the correct classification of cumulus resulting from lowering the standard deviation threshold used in the texture test from 0.25 to 0.05.

4. PRECIPITATION INTENSITY

Three precipitation areas (Fig. 5C) within the verification region are found in this case: the frontal boundary, the southwest quadrant and an area including eastern Florida and the intercoastal sections of Georgia and South Carolina. Precipitation is not verified over the ocean areas.

In Fig. 5C, the frontal boundary is clearly identified with estimates of light and moderate precipitation intensity which is in agreement with the surface reports and radar detection of rain and rain showers (Fig. 6). The earlier NPS analysis overestimated the precipitation intensity and areal coverage. Changing the infrared and visible thresholds defining precipitation from 251 K to 249 K and 0.31 to 0.55, respectively, produced a better precipitation analysis.

The precipitation analysis in the southwest quadrant is in agreement with the verification data for this region. Moderate to heavy showers are reported by radar.

Radar overestimates the amount and area of precipitation over eastern Florida and the intercoastal sections of Georgia and South Carolina. Precipitation is not identified by the satellite-derived analysis which is in agreement with the manual satellite analysis and surface observations which depict broken and scattered cumulus, altostratus and cirrus. A few radar-detected thunderstorms to the east of Florida are analyzed by the model.

5. CLOUD-TOP TEMPERATURE/HEIGHT

Cloud-top temperature and height results are presented in Figs. 5D and 5E. The NPS analysis of the cloud-top temperature

is not easily verified except through an independent upper-air analysis of individual plotted radiosonde soundings where temperatures are established at the analyzed top of the cloud layer. Cloud-top temperatures are appropriate for selected cloud types and bases, in that low clouds denote warmer temperatures whereas high clouds denote colder temperatures. Also, radar cloud tops from the ARS chart can be used for precipitating clouds. From this case two areas are designated for discussion: the frontal boundary and the region over the western Florida panhandle and southern Alabama.

Along the frontal boundary, the model indicates a range of cloud-top temperatures from 220 K to 280 K which agrees with the surface observations of a wide variety of cloud layers and types. Four of the six selected upper-air soundings were within the frontal zone; Wallops Island, Virginia, Greensboro, North Carolina, Athens, Georgia and Centreville, Alabama. The maximum cloud height variation from the NPS analysis to the upper-air verification data is 50 mb at Athens, Georgia and a minimum of 5 mb at Centreville, Alabama and Wallops Island, Virginia.

In the region over the western Florida panhandle, the NPS cloud-top temperature analysis shows a range of temperatures from 200 K to 280 K; this is verified by the surface data where observed cirrus, cumulonimbus and stratocumulus have cloud-top temperatures of 210 K, 220 K and 270 K, respectively. The area is largely covered by temperatures below 240 K indicating considerable amounts of high clouds, mostly cumulonimbus. The

surface observation from Mobile, Alabama reports cumulonimbus occurring at the station and to the west. The ARS chart indicates echo tops from 42,000 to 46,000 ft in the region.

The cloud-top height analysis (Fig. 5E) is a function of cloud-top temperature; therefore, it follows the cloud-top temperature pattern. The cloud-top height distribution in both regions agrees with the available verification data.

One additional region, east and northeast of the Bahama Islands is significant. The manual satellite analysis indicates a large area of overcast cumulonimbus. The NPS analysis depicts a range of cloud-top heights from 180 to 200 mb (70,000 ft to 40,000 ft) which is generally consistent with the manual satellite analysis depiction of cumulonimbus.

B. 11 AUGUST 1983

1. SYNOPTIC DESCRIPTION

In this second case, stronger synoptic systems are evident. A 1003 mb low pressure center is located over Lake Ontario. A cold front extends from the low through central Ohio, southern Indiana and Illinois, south-central Missouri and southern Kansas. A warm front extends from the low through northwestern New York, northern Pennsylvania and southern Connecticut (Figs. 8 and 9). An old cold vortex is west of the new system over Wisconsin. The Bermuda high extends over the southeastern United States.

2. CLOUD AMOUNT

The GOES images (Figs. 8 and 9), surface observations (Fig. 11) and NPS analysis (Fig. 10A) indicate clear and some scattered skies over Georgia, southern Alabama and Mississippi; the earlier analysis of this case depicted broken and scattered clouds. The clear slot immediately behind the cold front through south-central Indiana and Illinois is also analyzed correctly by the current NPS model.

The cloud amount estimation for overcast and clear skies is also accurate along the eastern coastal waters; the clear skies are verified by the surface observations (Fig. 11) and manual analysis (Fig. 12). Broken and scattered amounts are underestimated over the southeastern United States. Raising the cloud/no cloud threshold value eliminated the overestimation of overcast along the east coast that occurred in the Moren study.

3. CLOUD TYPE

The cloud type results indicate that the northeastern portion of the frontal zone is dominated by nimbostratus, altostratus and cirrus with cumulus congestus along the edges (Fig. 10B). The surface observations (Fig. 11) and manual analysis (Fig. 12) verify these classifications. In the far northwest portion of the cloud type analysis stratocumulus and cumulus are the dominant cloud types, and in the north central region the NPS analysis depicts nimbostratus/multi-layered clouds, an area of cumulonimbus and an area of broken altostratus. The manual satellite analysis and surface observations confirm these cloud types.

The NPS model identifies the cumulus and cirrus that exists in the prefrontal region which extends from western Virginia to northern Alabama and the cumulonimbus, multi-layered/nimbostratus and cirrus in the southern quadrants. The surface verification data and manual analysis confirm these cloud types.

4. PRECIPITATION INTENSITY

Precipitation is detected in the frontal region and in the southern quadrants since cumulonimbus and nimbostratus clouds are present in these two areas.

The frontal zone precipitation distribution and intensity estimation by the NPS model is accurate (Fig. 10C). All three intensities (light, moderate, heavy) are specified and the model

indicates the lack of precipitation over western Pennsylvania which is verified by the surface observations and ARS chart (Fig. 11). Moderate and heavy precipitation intensities and area coverage also concurs with the verification data in the southern quadrants.

5. CLOUD-TOP TEMPERATURE/HEIGHT

The NPS cloud-top temperature analysis indicates a range of temperatures along the frontal zone. As seen in Figs. 10D and 10E, the cloud-top temperature/height over Ohio is near 210 K/200 mb; this is in agreement with the radar measurements of cumulonimbus cloud-top heights ranging from 35,000 - 40,000 ft in this area (Fig. 11). In the region over Lake Michigan, the NPS model cloud-top temperatures range from 260 K to 290 K. This is confirmed by surface observations of low to middle clouds and the sounding cloud temperatures of 279 K (756 mb) at Green Bay, Wisconsin and 289 K (850 mb) at Flint, Michigan.

C. 23 AUGUST 1983

1. SYNOPTIC DESCRIPTION

In this third case a quasi-stationary front extends across central Virginia, southern West Virginia, Kentucky, western Tennessee and northeastern Arkansas. The Bermuda high does not ridge westward over the southeastern United States. A 1025 mb high pressure system over Canada advects modified polar air into the northern United States while a weak 1017 mb low pressure center is discernible over south-central North Carolina with troughing to the southwest. Cold, dry continental polar air (cP) flows into the northeastern United States as warm moist tropical air (mT) is advected weakly into the southern United States (Figs. 13 and 14).

2. CLOUD AMOUNT

The location of cloud masses, their orientation and amounts (Fig. 15A) are confirmed by the surface observations (Fig. 16) and manual analysis (Fig. 17). Some broken cumulus in the northeastern United States and Great Lakes region are classified as overcast in this case. Note the broken pattern of the overcast reports. Over Florida the automated analysis indicates scattered and broken conditions which is in agreement with the surface reports of scattered skies.

3. CLOUD TYPE

Four cloud type areas (Fig. 15B) are designated for discussion: the northwest quadrant, the frontal cloud type boundary, the northeast quadrant and the east central portion of the study region just off the Carolina coast.

The northwest quadrant has several different cloud types: embedded cumulus congestus, cirrus, altostratus and stratus. The current NPS analysis (Fig. 15B) is in agreement with the surface observations (Fig. 16) and manual analysis (Fig. 17); in the Moren study the cirrus was classified as cumulus congestus. The NPS analysis depicts the area over central Wisconsin, northern Illinois, Lake Michigan and southern Michigan as clear with some low clouds (cumulus and stratus). Thin cirrus is indicated by the surface observations and satellite imagery.

Along the frontal region, the NPS analysis identifies stratocumulus, cumulus and altostratus and cumulus congestus. The surface observations (Fig. 16) and manual satellite analysis (Fig. 17) confirm these cloud types. The earlier analysis overestimated cumulus congestus. Improvement in the cloud type classification along the frontal zone is due to changing the infrared temperature threshold differentiating stratocumulus and cumulus congestus from 271 K to 264 K and using a texture test to distinguish between altostratus and cumulus congestus. Thin cirrus observed south of the front over North Carolina, Tennessee and Virginia are not analyzed by the model.

In the extreme northeast quadrant and southern Florida, the verification data confirm the cloud-type classification of cumulus. In the east central portion of the study area, the NPS analysis depicts a broad area of nimbostratus/multi-layered clouds, cumulonimbus, with cirrus blowing off to the west; this is verified by the surface observations (Fig. 16).

4. PRECIPITATION INTENSITY

The NPS precipitation intensity analysis (Fig. 15C) depicts two large regions of precipitation. One region, east of the Bahamas in the southeast quadrant, cannot be verified due to its distance from the reporting radar station network. The region near the east coast of North Carolina is verified by the surface observations (Fig. 16) where a light rainshower is occurring at Cape Hatteras, North Carolina and a broad area of light intensity precipitation is indicated by the ARS analysis.

Three regions indicated on the surface observation and ARS verification chart are not depicted by the NPS analysis; an area of moderate precipitation over Maryland, northern Virginia and West Virginia, an area of light precipitation over western and southern Illinois and southern Indiana, and an area of light precipitation over southern Florida.

In each case, stratocumulus, altostratus and cumulus congestus are analyzed and the precipitation infrared temperature threshold was not reached. The infrared values for these areas are just below the 249 K precipitation/no precipitation threshold. This is illustrated by the cloud-top temperature analysis (Fig. 15D) where a few colder cloud-top temperatures in the region correspond to the radar-detected precipitation areas.

5. CLOUD-TOP TEMPERATURE/HEIGHT

Two regions from the NPS cloud-top temperature analysis (Fig. 15D) are identified for discussion: a region over northern Virginia, western Maryland, southern Pennsylvania and northern West Virginia and a region over Florida.

In the first region, the NPS analysis depicts a range of values from 240 K to 280 K which corresponds to an upper-air sounding temperature of 266 K at Washington-Dulles, Virginia. The surface observations (Fig. 16) in this region indicate multi-layered low, middle and high clouds, inferring a broad range of cloud-top temperatures.

In the region over Florida cloud-top temperatures range from 270 to 280 K. These temperatures, which are indicative of low cumulus (corresponding to the cloud-top height analysis in Fig. 15E) are verified by both the satellite manual analysis and surface observations.

D. 31 AUGUST 1983

1. SYNOPTIC DESCRIPTION

In the 31 AUG case a weak 1011 mb closed low is centered over New Hampshire. A cold front extends from the low through southeastern New York, east central Pennsylvania and central West Virginia to a 1012 mb low over northern Kentucky continuing to a weak 1012 mb low over western Tennessee/western Arkansas. A weak 1011 mb low is centered at 28N 87.5W in the Gulf of Mexico and a 1022 mb high is centered over northwestern Wisconsin (Figs. 18 and 19). Modified continental polar air (cP) is being slowly drawn into the north-central United States while maritime tropical air (mT) is being advected across the Florida panhandle. The frontal boundary is weakly defined in the surface data.

2. CLOUD AMOUNT

The cloud amount analysis for this case is generally accurate. The overcast areas (Fig. 20A) in the frontal region and in the convective areas to the southeast are verified by the surface observations (Fig. 21) and manual analysis (Fig. 22). The regions over north-central South Carolina/southeast North Carolina and southeast Indiana that were analyzed incorrectly in the Moren study as overcast are now depicted as clear to scattered skies with the scattered conditions underestimated. The scattered and clear skies over the Great Lakes region are also depicted well.

3. CLOUD TYPE

Two cloud type areas are designated for verification: the frontal boundary and an area in the east-central and southern

quadrants. In the eastern portion of the frontal boundary, the NPS analysis (Fig. 20B) depicts altostratus, nimbostratus and cirrus. In the extreme northeast region, stratocumulus and cumulus are classified. Along the central portion of the frontal zone, the NPS analysis indicates more multi-layered/nimbostratus, altotratatus, and cirrus, with some cumulus throughout this area. The western frontal region is dominated by cumulus and stratocumulus clouds. The verification data (Figs. 21 and 22) support the model analysis of the frontal boundary (Fig. 6). The satellite data depict a rich variety of cloud structure in the frontal zone.

In the east central quadrant, the cloud type analysis indicates cirrus (earlier analyzed incorrectly as altostratus) and cumulus. The satellite images (Figs. 18 and 19), manual satellite analysis (Fig. 22) and surface observations (Fig. 21) verify this analysis. The cumulonimbus, cumulus congestus and cumulus in the southern quadrant over Florida are also in agreement with the verification data.

4. PRECIPITATION INTENSITY

There are three main precipitation areas in this case; along the frontal boundary and in the western and southern quadrants. As seen in Fig. 20C, the entire frontal region in the NPS analysis depicts light to moderate precipitation intensity which is verified by the surface observations and ARS chart (Fig. 21).

In the western quadrant the NPS model analyzes light to moderate precipitation. Although the ARS chart does not verify

this precipitation, there are reports of occasional light rain from the surface stations. The intensity of the precipitation may have been too light for radar detection.

In the southern quadrants the NPS precipitation analysis shows moderate to heavy rainfall which is also verified by the ARS chart. Each of the three precipitation regions and their intensities are defined accurately by the model.

5. CLOUD-TOP TEMPERATURE/HEIGHT

The NPS cloud-top temperature/height analyses over the regions of central and northern Ohio/western Kentucky are discussed because these areas encompass a broad range of cloud types.

The cloud-top temperature analysis (Fig. 20D) over northern Ohio/western Pennsylvania depicts a range of cloud-top temperatures from 220 K to 280 K. The GOES infrared satellite imagery shows a sharply-defined bright area over northern Ohio inferring very cold cloud-top temperatures. The 263 K cloud-top radiosonde observation at Pittsburgh, Pennsylvania is in agreement with the 260 K NPS cloud-top temperature analysis.

In the region over Tennessee/western Kentucky the cloud-top temperature analysis shows a range of temperatures from 220 K to 280 K which corresponds to the surface reports of a broad range of middle and high clouds in this region. A Nashville, Tennessee sounding cloud-top temperature of 268 K agrees with the 270 K cloud-top temperature of the NPS analysis. The NPS cloud-top height analysis (Fig. 20E) follows the cloud-top temperature analysis.

E. 02 SEPTEMBER 1983

1. SYNOPTIC DESCRIPTION

In this final case a 1010 mb low is centered over northeastern Florida. A 1020 mb high is located over central Pennsylvania and cold moist air from the east of the high and warm moist air from the open low and the Bermuda high are directed westward to the central eastern seaboard. A front is moving into the northern Great Lakes area (Figs. 23 and 24).

2. CLOUD AMOUNT

The southeast and northwest quadrants and the central quadrants of the cloud amount analysis are discussed. The earlier cloud amount analysis depicted scattered and broken conditions in the southeast and northwest quadrants while the current analysis (Fig. 25C) indicates clear to scattered conditions which is in agreement with the satellite images, surface observations (Fig. 26) and manual analysis (Fig. 27). The large cloud-covered region is depicted as overcast with some scattered and clear holes; the verification data shows some broken and scattered skies within the general cloud structure of the weather system located in southeastern United States.

3. CLOUD TYPE

Two cloud type areas are discussed: the frontal boundary and the Great Lakes region. In the eastern region of the frontal boundary, which is aligned ENE to WSW, the model identifies nimbostratus/multi-layered clouds, cumulonimbus, cumulus congestus and cirrus (analyzed earlier as altostratus) on the edges (Fig. 25B); the western region of the frontal cloudiness is

depicted as cumulus and stratocumulus. The surface observations (Fig. 26) and manual satellite analysis (Fig. 27) verify these cloud types. The various cloud type regions within this major cloud system are clearly illustrated in this case.

In the Great Lakes region the cloud type analysis indicates nimbostratus/multi-layered clouds, cumulonimbus and cirrus to the south. The verification data supports the cloud type analysis; surface observations of cumulonimbus, multiple-cloud layers and cirrus are reported in this region.

4. PRECIPITATION INTENSITY

Precipitation is associated with the large multiple-layered cloud system and the small cloud mass in the extreme north central area. Over the eastern and southern quadrants encompassing the broad cloud mass, the precipitation analysis (Fig. 25C) depicts precipitation intensities ranging from light to heavy. Although the intensities are overestimated, the precipitation areal boundaries are consistent with the surface observations and radar (Fig. 26). The model identifies the thunderstorms over Florida especially well. In the extreme north central region the model depicts moderate to heavy precipitation intensities which are verified by the radar which also detects thunderstorms in this region.

5. CLOUD-TOP TEMPERATURE/HEIGHT

Two regions are used to evaluate the cloud-top temperature/height analysis: the western section of the large cloud mass and a region east of the Florida/Georgia coastline.

In western section of Fig. 25D , cloud-top temperatures range from 260 K to 280 K corresponding to low clouds cumulus and stratocumulus. The upper-air sounding temperature at Nashville, Tennessee indicates a cloud-top temperature of 268 K at 700 mb which compares well with the NPS cloud-top temperature analysis.

In the region east of the Florida/Georgia coastlines, a minimum cloud-top height of 200 mb (210 K) is indicated by the model (Fig. 25E). This is verified by the manual satellite analysis (Fig. 27) , which depicts large cumulonimbus clouds in this area.

V. Statistical Evaluation Plan

A statistical evaluation of cloud type and precipitation detection is performed on each case. For each case, approximately 75 surface reports, the majority being located in the eastern and southern quadrants of the study region, are used in the evaluation. Each surface observation is compared to a 5 x 5 (20 x 20 n mi) matrix containing satellite data. A voting procedure is used on the 5 x 5 satellite matrix to determine the dominate cloud type and whether there is precipitation occurring over the 5 x 5 pixel area. A straight percentage is computed for the number of agreements between the surface observation and the satellite information assuming the surface data are correct: $\text{PERCENT CORRECT} = \text{NUMBER OF AGREEMENTS} / \text{TOTAL NUMBER}$. This percentage correct is calculated for clear conditions and eight cloud type categories (cirrus, altostratus, stratus, stratocumulus, cumulus, cumulus congestus, nimbostratus and cumulonimbus) as well as for surface reports of precipitation and no precipitation. Surface reports of multi-layered clouds are evaluated differently since the NPS cloud routine does not separate multi-layered and nimbostratus clouds.

The surface observations of sky cover, present weather, low cloud type and high cloud type are used to determine the cloud type from the surface reports. If both the cloud information and present weather are missing, the surface report is ignored. If just the cloud information is missing, but present weather exists, the cloud type is determined by the present weather. For example, if the cloud type information is missing, but fog is observed, the cloud type decision is stratus. If the sky cover

is less than three tenths, the report is classified as clear. If only a low cloud type is reported, then stratus, stratocumulus, cumulus, cumulus congestus or cumulonimbus is the result. Reports of only middle clouds are classified as either nimbostratus or altostratus depending upon whether there is precipitation (nimbostratus) occurring. If only high clouds are reported, the cloud type decision is cirrus. If two or more cloud types are observed, then the surface report is multi-layered clouds.

The satellite cloud types are determined by the visible and infrared digital data. Cloud types of cirrus, altostratus, stratus, stratocumulus, cumulus, cumulus congestus, nimbostratus and cumulonimbus are classified according to pre-established thresholds. Refer to the discussion in Chapter 2 and Fig. 1a. Multi-layered clouds are included in the nimbostratus cloud classification.

The surface cloud type information is compared to the result of the voting procedure used on the 5 x 5 satellite matrix corresponding to that surface station. The cloud type that occurs most frequently in the 5 x 5 satellite matrix is chosen as the predominant cloud type. For each cloud type classification, a percentage correct is computed.

Since no distinction is made in the satellite model between nimbostratus and multi-layered clouds, the surface reports of multiple cloud layers have to be evaluated in a different way. A comparison is made between the 5 x 5 satellite matrix corresponding to the surface report of multi-layered clouds; all

twenty-five cloud-typing decisions of the matrix are examined.

Surface reports of multiple layers are placed into five separate categories according to the thickness properties of the cloud types reported. Reports of dense cloud types at two or more levels are considered multi-layered (ML). Thin or transparent cloud types at upper and/or middle levels, but thick or opaque at the lower level are considered low clouds (CL). Transparent upper and/or lower layer cloud types, but opaque middle cloud types are considered middle clouds (CM). Thin middle and/or lower level cloud types, but dense clouds at upper levels are considered high clouds (CH). Surface reports of transparent cloud types at two or all three levels are classified as thin clouds (THIN).

Each 5 x 5 satellite matrix corresponding to a surface report of multi-layered clouds is categorized in a similar manner. If two or more cloud types appear at different levels, the satellite cloud-typing decision is considered to be multi-layered (ML). If the matrix contains a majority of zero values (a zero value indicates clear conditions), the resulting categorization is thin (THIN). The matrix is classified as low cloud type (CL) if the majority of the twenty-five pixels are low cloud types such as cumulus, stratus, stratocumulus, cumulus congestus and cumulonimbus. The cloud-typing decision is middle cloud (CM) if the satellite matrix contains predominately middle clouds (altostratus, nimbostratus). Finally, if the majority of cloud types are cirrus, the satellite cloud-typing decision is high cloud (CH).

The surface categorization of multi-layered clouds is

compared to the satellite classification. If there is a disagreement between the surface and satellite classifications, the multi-layered report is labelled mismatch.

The surface observation of present weather is used to determine whether precipitation is occurring at the time of the observation. The satellite precipitation/no precipitation decision is based on pre-established threshold values of digital visible and infrared data. Refer to the discussion in Chapter 2 and Fig. 1b.

The surface report of precipitation/no precipitation is compared to the result of the voting procedure used on the 5 x 5 satellite matrix. Twelve or more votes out of twenty-five for precipitation results in a decision of precipitation; less than twelve indicating no precipitation. Each surface report of precipitation is compared to the satellite decision and a percent correct is calculated. The same evaluation procedure is used for surface reports of no precipitation.

Direct comparison between ground-observed sky conditions and satellite digital data is a difficult task. An observer reports sky conditions that may cover a larger area than the satellite's field of view. Therefore, a disagreement between a synoptic station and a satellite classification may result. Secondly, an observer's cloud type classification is more subjective than a satellite's since the observer sees clouds at different angles. Furthermore, there is a difference in perspective between the surface observer and the satellite. The observer views the clouds from below, whereas the satellite senses from above.

These difficulties have a strong impact on the statistical results.

Many times there are two predominate cloud types at the same level that occur in the satellite matrix. Only the most frequently-occurring cloud type is used to compare to the surface report. Several times the verifying surface cloud type is the second most frequently-occurring cloud type. This also has a bearing on the cloud type statistics which are presented in the following chapter.

VI. Statistical Evaluation Results

The statistical evaluation of cloud type classification and precipitation occurrence produced similar results for all five case studies. Tables 2 and 3 list the evaluation results of the single and multiple cloud type classifications, respectively; the precipitation occurrence results appear in Table 4.

The success of the cloud/no cloud threshold is given by the classification accuracy of clear sky percentage correct statistics which range from 67% in the 31 AUG case to 100% in the 02 AUG and 23 AUG cases (Table 2). The low success percentage of the 31 AUG and 02 SEP cases is due to edges of small cumulus located near stations reporting clear skies; the predominate cloud type in the satellite matrix is cumulus, with clear skies as the second most frequently-occurring category.

The more successful pure cloud-type classifications are cloud types with uniform or smooth textures such as nimbostratus, stratocumulus, stratus and altostratus. Since these stratiform-type clouds often fill the satellite's field of view as well as cover the entire sky, the problem of classification with partially-filled field of views is minimized. The total percentage correct values for nimbostratus, stratocumulus, stratus and altostratus are 54%, 36%, 27% and 25%, respectively (Table 2).

The disagreement in the nimbostratus category for the 02 SEP case occurs with surface-observed nimbostratus that are analyzed as altostratus by the model. The nimbostratus/altostratus boundary lies near many of the synoptic stations. Even though nimbostratus occurs frequently in the satellite matrix,

altostratus may be the predominate cloud type.

Most of the stratocumulus classification error stems from large brightness standard deviations (greater than 0.05) which produce a satellite classification of cumulus rather than stratocumulus. The stratocumulus cloud edges are often located near synoptic stations which results in the larger brightness standard deviations.

The stratus classification error stems from two problems. For two reports of stratus the satellite detects an infrared temperature (i.e. 264 K) colder than the upper stratus threshold 276 K (Fig. 1a); the model indicates cirrus clouds. For the remainder of stratus cases the satellite detects brighter albedo values than the upper threshold limit for stratus (0.55), causing clouds to be classified as stratocumulus rather than stratus. There is no separation between stratus and stratocumulus in the visual as suggested in Liljas (1982).

The majority of synoptic reports of altostratus are in the category of altocumulus occurring with altostratus or nimbostratus. Since no precipitation is occurring at the time of the observation, these surface reports are classified as altostratus; the satellite analysis depicts nimbostratus. Therefore, a classification error results due to a misleading synoptic cloud type category that includes both altostratus and nimbostratus cloud types.

The less successful pure cloud-type classifications are clouds with nonuniform or rough textures such as cirrus, cumulus, cumulus congestus and cumulonimbus. Only one out of a total of

twenty-eight surface observations of cirrus and one out of five cumulus reports are analyzed correctly by the model (Table 2). The model fails to classify cumulus congestus and cumulonimbus. The incorrect cloud type classification by the satellite cloud-typing module is due to either satellite-measured infrared temperatures that are too warm or albedo values that are too dim.

The majority of misclassifications of cirrus and cumulonimbus clouds are due to satellite infrared temperatures exceeding the infrared thresholds. Many of the surface reports of cirrus, cirrostratus and cirrocumulus are described as thin high clouds and have extremely warm satellite infrared temperatures. These satellite infrared measurements exceed the 276 K threshold, producing erroneous low cloud classification. Due to the thin structure of the cirrus-type clouds, surface radiation is detected by the satellite through the cloud causing the warm infrared temperatures; therefore, these cirrus regions are misclassified as either clear skies or cumulus clouds depending upon the albedo values. This is especially evident in the 02 SEP case where only one out of sixteen surface reports of cirrus is in agreement with the cloud type analysis; the majority of the cirrus reports are semitransparent. Dense cirrus are classified correctly since they behave more like blackbodies. If cirrus albedos and temperature statistics could be separated from low cloud values, a value of cirrus emissivity could be used and more accurate cirrus typing achieved.

The four surface reports of cumulonimbus have warmer infrared temperatures (i.e. 250 K) than the expected 225 K threshold;

therefore, the NPS cloud-typing module classifies the cumulonimbus clouds as cumulus congestus or nimbostratus.

The majority of misclassifications of cumulus are due to pixels that have albedo values less than the cloud/no cloud threshold 0.17 (Fig. 1a). The satellite cloud-typing routine denotes the cumulus regions as clear. The success in classifying cumulus depends upon the satellite resolution. The small cumulus are not resolved with coarse resolution. Better results would be obtained if the cloud-typing decision was performed on each individual cloud pixel. Most surface reports of cumulus congestus are analyzed as cumulus. Both visible and infrared satellite-measured values are less than the 0.55 and 264 K thresholds, respectively.

The majority of the verification surface reports are of multiple cloud layers. 88% of the satellite decisions are in agreement with the surface categorizations (Table 3). Percent correct values for each individual case range from 97% in the 02 AUG case to 58% in the 11 AUG case. In the 02 AUG case, of the thirty-four multi-layered cloud reports there are seventeen of type ML, eight of type THIN, six of type CL, one of type CH and CM and only one mismatch. In the 11 AUG case, the majority of mismatches correspond to surface observations of multi-layered clouds with dense low and high level clouds while the corresponding satellite estimate is multiple layers with dominant nimbostratus clouds. The satellite analysis indicates a large dense cloud mass and is unable to distinguish between the different layers.

The statistical evaluation results are reasonable for both precipitation and no precipitation cases. The percent correct values for the FAIR classification range from 86% in the 02 SEP case to 98% in the 23 AUG case (Table 4). Percent correct values for the RAIN classification range from 50% (11 AUG) to 100% (23 AUG).

Two types of precipitation classification errors can occur: A surface observation of precipitation is classified as a non-precipitating region by the model or a report of no precipitation is analyzed as a precipitating region. In the first case, the visual and infrared values are below the precipitation/no precipitation thresholds of 0.55 and 249 K, respectively. In the second case, the albedo and temperature used in making the precipitation decision exceed the thresholds.

Each of the five cases show similar statistical results. The success of the clear sky percentage correct statistics indicate that 0.17 is a representative cloud/no cloud threshold. The more successful pure cloud type classifications are for cloud types with uniform textures such as nimbostratus, stratocumulus, stratus and altostratus. Classification errors are due to cloud type boundaries, brightness standard deviations, cold infrared temperatures and bright visible albedos and misleading synoptic cloud description categories. The less successful pure cloud type classifications are for clouds with nonuniform textures such as cirrus, cumulus, cumulus congestus and cumulonimbus. Misclassifications are due to warm infrared temperatures and low albedos. The majority of multi-layered cloud systems are analyzed correctly. Satellite-surface disagreements occur with

surface observations of dense low and high clouds that the satellite senses as thick middle cloud. The majority of precipitation statistics for both FAIR and RAIN classifications are encouraging. The only classification errors occur when the infrared and visible values are above (below) the precipitation/no precipitation thresholds.

VII. Summary and Conclusions

The use of digital satellite data offers the opportunity to improve our analysis of a variety of weather phenomena and produce enhanced operational analysis products.

A cloud and precipitation analysis program using satellite digital data was developed for an interactive mini-computer system. The program uses digital (visual and infrared) geostationary satellite data from the GOES System as well as operational upper-air and surface temperature profiles. From this collection of data, the program produces analyses of cloud amount, cloud type, cloud-top temperature, cloud-top height and precipitation intensity.

Verification of the program was conducted using five summer cases of GOES-East data for a region over the eastern United States and northern west Atlantic Ocean. Reasonable results were obtained from the synoptic subjective evaluations performed on each case. The majority of cloud and precipitation analyses correctly characterized the mesoscale cloud and weather features. Less successful results were obtained from the single station-satellite data comparison used on the cloud type and precipitation parameters.

Cloud amount estimates of overcast and clear skies were generally accurate using a 0.17 cloud/no cloud threshold. Some clear skies were classified as cumulus since the edges of small cumulus were located near synoptic stations. Broken and scattered conditions were underestimated due to the size of the array of satellite data used to compute cloud amount.

The cloud type analyses depicted the general cloud patterns.

Most cloud types were analyzed correctly after the modifications to the model were made based on Moren's (1984) evaluation. More classification errors were illustrated in the direct comparison between the satellite data and single station observations. Uniform cloud types, nimbostratus and stratocumulus were classified correctly 54% and 36% of the time, respectively. Most nimbostratus classification errors were due to nimbostratus/altostratus boundaries located near the verification station; surface observations of nimbostratus were classified as altostratus by the model. The majority of misclassifications of stratocumulus were due to errors in the texture decision; stratocumulus was analyzed as cumulus since the standard deviations were greater than 0.05. Less successful results were obtained for the uniform-textured cloud types stratus (27% correct) and altostratus (25% correct) in which classification errors were due to cold infrared temperatures/bright visible albedos and a misleading synoptic cloud description, respectively. The following classification errors occurred with nonuniform-textured cloud types such as: (1) small cumulus which were smaller than the satellite sensor's field of view; (2) thin cirrus which allow surface radiation to be transmitted to the sensor; and (3) cumulus congestus and cumulonimbus which were warmer than their respective thresholds. 88% of the multi-layered cloud systems were analyzed correctly. The only satellite-surface disagreement occurred with surface reports of dense low and high clouds that were depicted as dense middle cloud by the model.

The majority of precipitation analyses were successful, especially for cold and bright precipitating clouds. 93% of the surface reports of fair skies and 67% of the precipitation reports were analyzed correctly by the model. The only analysis errors occurred when the infrared and visible values were above (below) the precipitation/no precipitation thresholds with surface observations of clear skies (precipitation).

The majority of cloud-top temperature/height analyses were representative of the cloud types and patterns in each case. Most cloud-top soundings verified the analyzed cloud-top temperatures.

The evaluation results of the five cases illustrate that satellite digital data can be used as an effective tool for describing mesoscale and sub-synoptic weather features.

LIST OF REFERENCES

- Corbell, P., C. Callahan and W. J. Kotsch, 1978: The GOES/SMS Users Guide, NOAA National Environmental Satellite Service, (Ref App II Attachment A3).
- Fye, F. K., 1978: The AFGWC automated cloud analysis model. AFGWC Technical Memorandum 78-102, H.Q. Air Force Global Weather Central, Offutt AFB, Nebraska, 97 pp.
- Keegan, T.J. and Niedzielski, 1981: Specification of cloud amount over local areas from GOES visual imagery. AFGL-TR-81-0153, 61 pp.
- Harris, R. and E.C. Barrett, 1978: Toward an objective neph-analysis. J. Appl. Meteorol., 17, 1258-1266.
- Liljas, E., 1982: Automated techniques for the analysis of satellite cloud imagery. Nowcasting, ed. K. Browning, Academic Press, 177-190.
- Moren, C., 1984: Evaluation of the SPADS automated cloud analysis model. M.S. Thesis, Naval Postgraduate School, 139 pp.
- Muench, H. S. and T. J. Keegan, 1979: Development of techniques to specify cloudiness and rainfall rate using GOES imagery data. AGFL-TR-79-0255, AD A084, 757 pp.
- National Oceanic and Atmospheric Administration, U.S. Department of Commerce, 1979: Technical Procedures Bulletin: The Radar Guidance Program, 253, (23 January, 1979).
- Nelson, C. A., 1982: Estimation and mapping of cloud and rainfall areas with an interactive computer. M.S. Thesis, Naval Postgraduate School, 134 pp.
- Reynolds, D. W. and T. H. VonderHaar, 1977: A bispectral method for cloud parameter determination. Mon. Wea. Rev., 105, 446-457.
- Tsonis, A.A., 1984: On the separability of various classes from GOES visible and infrared data. J. Appl. Meteor., 23, pp. 1393-1410.
- Wyse, N., 1984: The inclusion of surface data into the SPADS cloud analysis model. M.S. Thesis, Naval Postgraduate School, 177 pp.

APPENDIX A

TABLES

Table 1. Cloud/precipitation grayshade categories in order of decreasing brightness.

<u>Cloud Amount</u>		<u>Precipitation Intensity</u>
1. OVC	100% cloud cover	1. 3 Heavy
2. BRO	75% cloud cover	2. 2 Moderate
3. SCA	50% cloud cover	3. 1 Light
4. SCA-CLR*	25% cloud cover	
* SCA-CLR category is not distinguishable		

<u>Cloud Type</u>	
1. Cb	cumulonimbus
2. Ns	nimbostratus
3. Cu Cong	cumulus congestus
4. Cu	cumulus
5. Sc	stratocumulus
6. St	stratus
7. As	altostratus
8. Ci	cirrus

<u>Cloud-Top Temperature</u>		<u>Cloud-Top Height</u>	
1. 210	210-219 K	1. 100	100-199 mb
2. 220	220-229 K	2. 200	200-299 mb
3. 230	230-239 K	3. 300	300-399 mb
4. 240	240-249 K	4. 400	400-499 mb
5. 250	250-259 K	5. 500	500-599 mb
6. 260	260-269 K	6. 600	600-699 mb
7. 270	270-279 K	7. 700	700-799 mb
8. 280	280-289 K	8. 800*	800-899 mb
9. 290*	290-300 K	9. 900*	900-1000 mb

* 290 category is considered as surface value so it is black

* 800 & 900 categories are not distinguishable

Table 2. Statistical evaluation results of single cloud types.

	02 AUG	11 AUG	23 AUG
<u>Cloud Type</u>			
CLEAR	24/24=100%	34/35=97%	17/17=100%
CIRRUS	1/2=50%	0/3	0/7
ALTOSTRATUS	0/1	0/4	1/3=33%
STRATUS	0/2	1/3=33%	0/1
STRATOCUMULUS	0/4	8/9=89%	1/5=20%
NIMBOSTRATUS	no report	4/6=67%	1/1=100%
CUMULUS	0/1	no report	no report
CUMULUS CONGESTUS	0/4	0/2	no report
CUMULONIMBUS	no report	0/3	no report

	31 AUG	02 SEP	Total for all five cases
<u>Cloud Type</u>			
CLEAR	4/6=67%	34/38=89%	109/121=90%
CIRRUS	0/1	1/16	1/28
ALTOSTRATUS	2/4=50%	0/1	3/12=25%
STRATUS	1/4=25%	1/3=33%	3/11=27%
STRATOCUMULUS	1/11=10%	2/4=50%	13/36=36%
NIMBOSTRATUS	no report	3/8=38%	7/13=54%
CUMULUS	1/4=25%	no report	1/5=20%
CUMULUS CONGESTUS	0/2	no report	0/8
CUMULONIMBUS	no report	0/1	0/4

Table 3. Statistical evaluation results of multi-layered clouds.

	02 AUG	11 AUG	23 AUG
<u>Percentage of satellite-surface agreement</u>	33/34=97%	15/26=58%	29/31=94%
<u>Percentage of satellite-surface mismatched</u>	1/34=3%	11/26=42%	2/31=6%
<u>Number of occurrences in specific multi-layered category</u>			
ML	17/34	4/26	7/31
THIN	8/34	2/26	14/31
CL	6/34	2/26	6/31
CM	1/34	6/26	1/31
CH	1/34	1/26	1/31
	31 AUG	02 SEP	Total for all five cases
<u>Percentage of satellite-surface agreement</u>	30/32=94%	23/25=92%	130/148=88%
<u>Percentage of satellite-surface mismatched</u>	1/34=3%	11/26=42%	8/148=12%
<u>Number of occurrences in specific multi-layered category</u>			
ML	14/32	8/25	50/148
THIN	7/32	2/25	33/148
CL	3/32	3/25	20/148
CM	6/32	6/25	20/148
CH	0/32	4/25	7/148

Table 4. Statistical evaluation results of precipitation occurrence.

	02 AUG	11 AUG	23 AUG
<u>Category</u>			
RAIN	none	4/8=50%	1/1=100%
FAIR	69/72=96%	78/84=93%	60/61=98%
	31 AUG	02 SEP	Total for all five cases
<u>Category</u>			
RAIN	2/3=67%	7/9=78%	14/21=67%
FAIR	56/61=92%	74/86=86%	337/364=93%

APPENDIX B

FIGURES

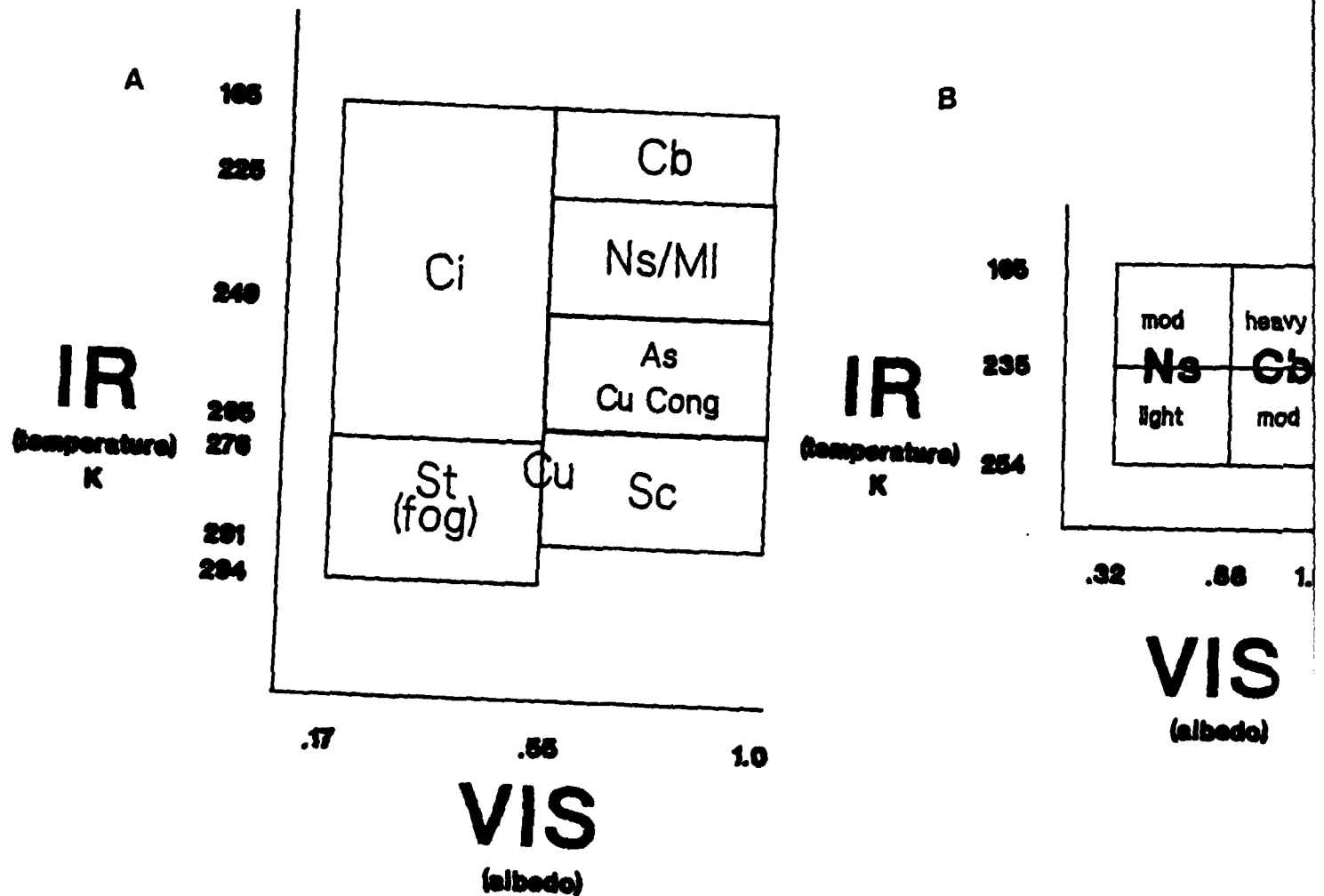


Fig. 1a) Two-dimensional cloud typing graph using GOES IR and VIS satellite digital data; b) Two-dimensional precipitation histogram using GOES IR and VIS digital satellite data.

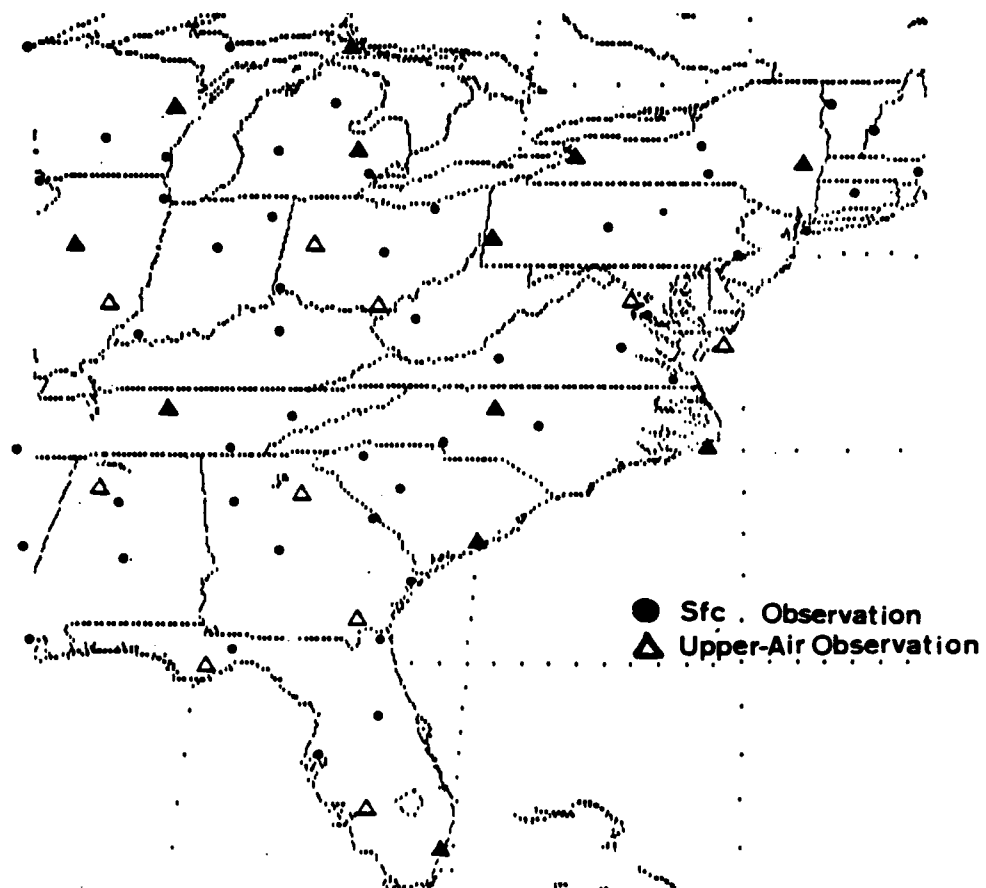


Fig. 2. Geographic location of study region

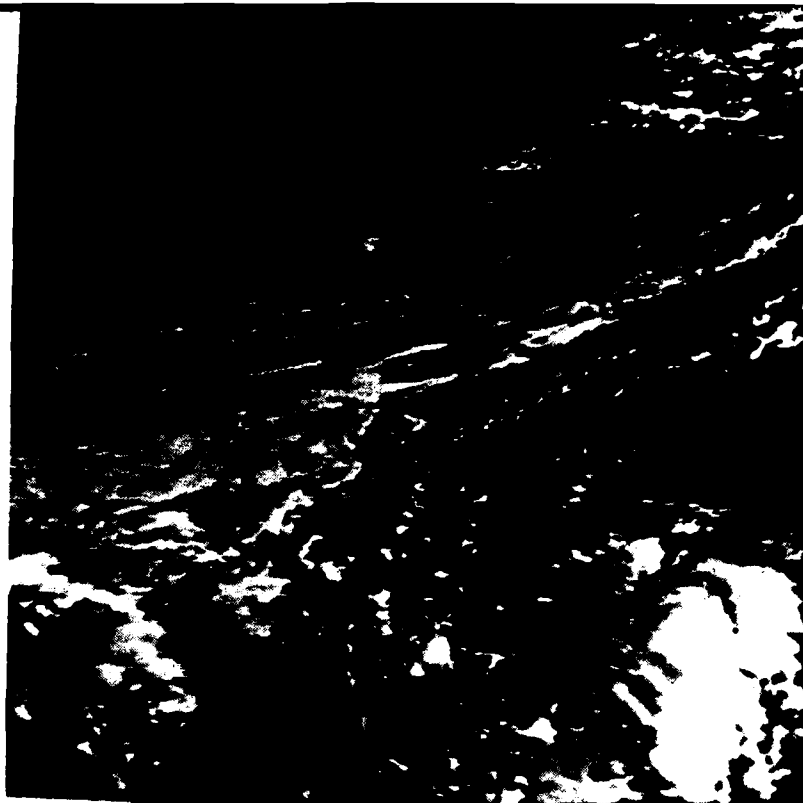


Fig. 3. GOES VIS imagery for 02 AUG 83

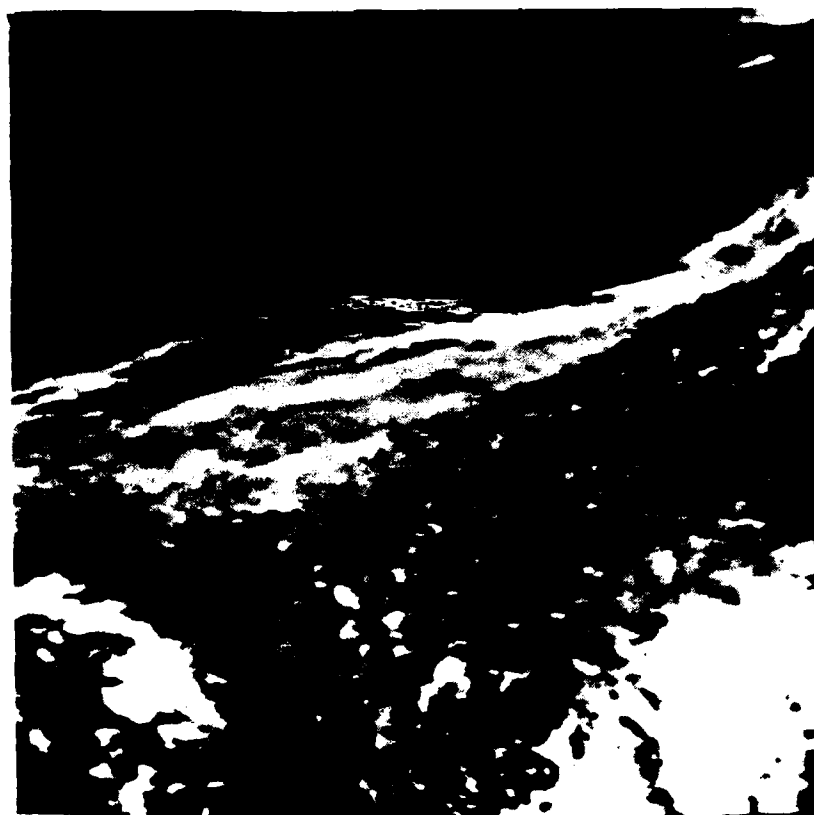


Fig. 4. GOES IR imagery for 02 AUG 85



Fig. 5A. Cloud amount analysis for 02 AUG 83.
4 grayshades are used to distinguish
between cloud amounts: 100% cloud cover (OVC),
lightest grayshade; 75% cloud cover (BRO),
medium grayshade; 50% cloud cover (SCA),
darkest visible grayshade; 25% cloud cover
(CLR-SCA), darkest grayshade (unable to
distinguish on photo).



Fig. 5B. Cloud type analysis for 02 AUG 83. Eight grayshades are used to illustrate eight different cloud types. Cloud types in decreasing order of grayshade brightness are as follows: cumulonimbus (Cb), brightest grayshade; nimbostratus (Ns); cumulus congestus (Cu Cong); cumulus (Cu); stratocumulus (Sc); stratus (St); altostratus (As); cirrus (Ci), darkest grayshade.

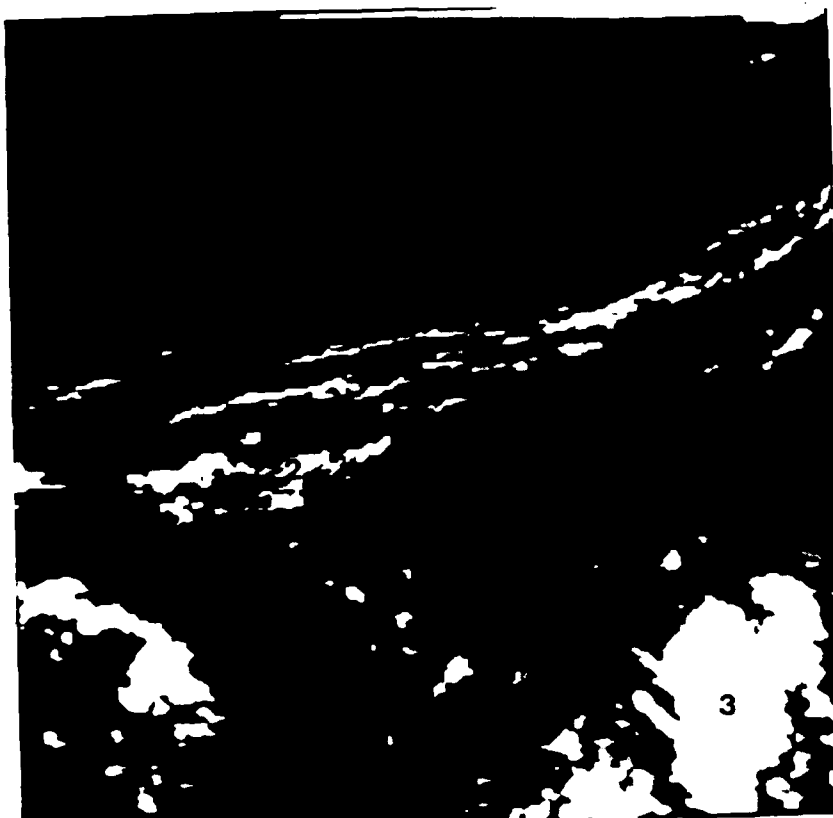


Fig. 5C. Precipitation intensity analysis for 02 AUG 83.
Three grayshades are used to distinguish between
precipitation intensities: heavy (3), bright-
est grayshade; moderate (2), medium grayshade;
light (1), darkest grayshade.



Fig. 5D. Cloud-top temperature analysis for 02 AUG 83. Nine grayshades are used to illustrate 10 K intervals of cloud-top temperatures. Cloud-top temperature 10 K intervals in order of decreasing grayshade brightness are as follows: 210-219 K, brightest grayshade; 220-229 K; 230-239 K; 240-249 K; 250-259 K; 260-269 K; 270-279 K; 280-289 K, darkest visible grayshade; 290-300 K, surface value which correspond to a black background.

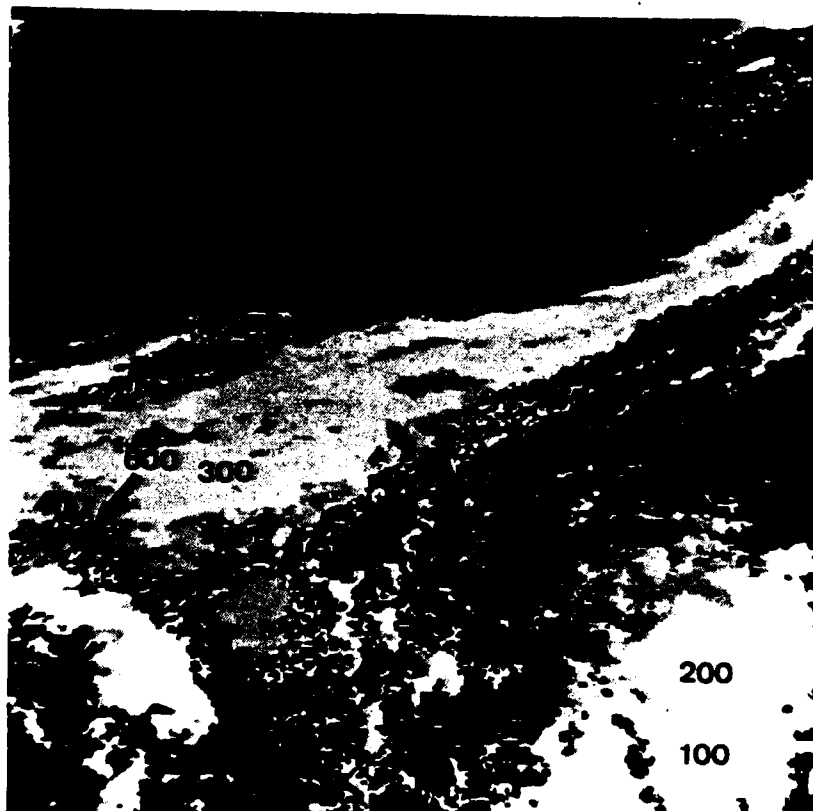


Fig. 5E. Cloud-top height analysis for 02 AUG 83. Nine grayshades are used to illustrate 100 mb cloud-top height intervals. Cloud-top height 100 mb intervals in order of decreasing grayshade brightness are as follows: 100-199 mb, brightest grayshade; 200-299 mb; 300-399 mb; 400-499 mb; 500-599 mb; 600-699 mb; 700-799 mb, darkest visible grayshade; 800-899 mb (unable to distinguish on photo); 900-1000 mb, darkest grayshade (unable to distinguish on photo).



Fig. 6. Surface observation and ARS verification chart for 02 AUG 83



66

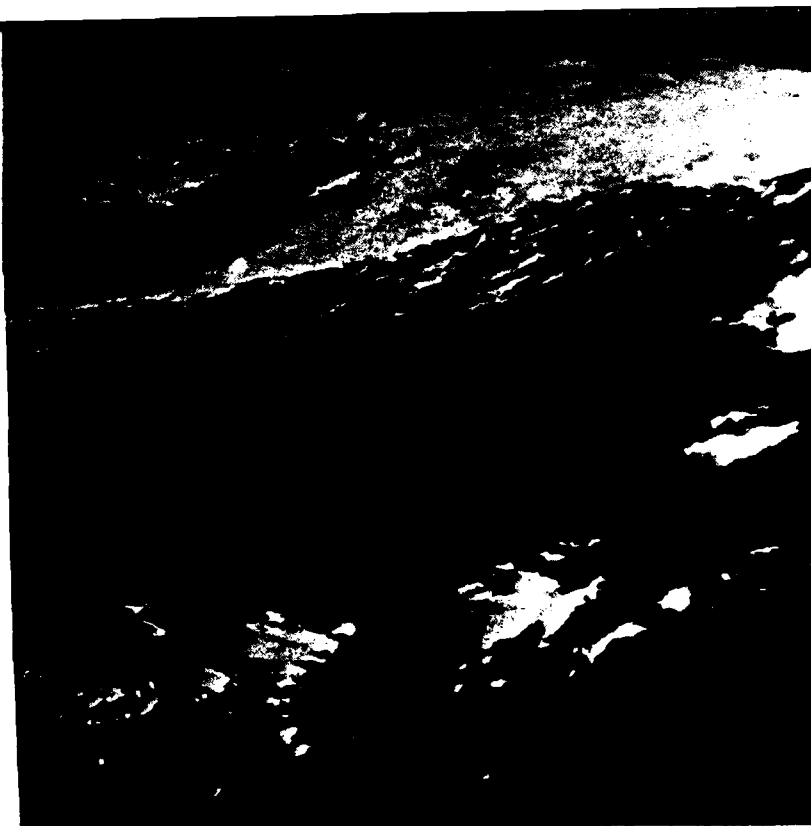


Fig. 8. GOES VIS imagery for 11 AUG 83.

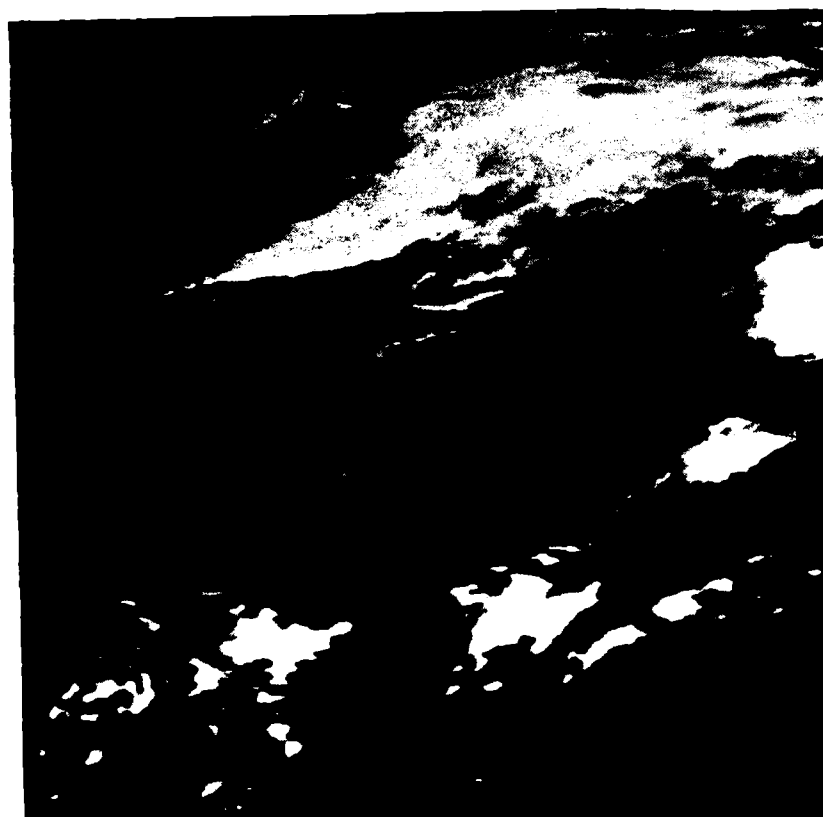


Fig. 9. GOES IR imagery for 11 AUG 83.



Fig. 10A. Same as Fig. 5A except for 11 AUG 83.

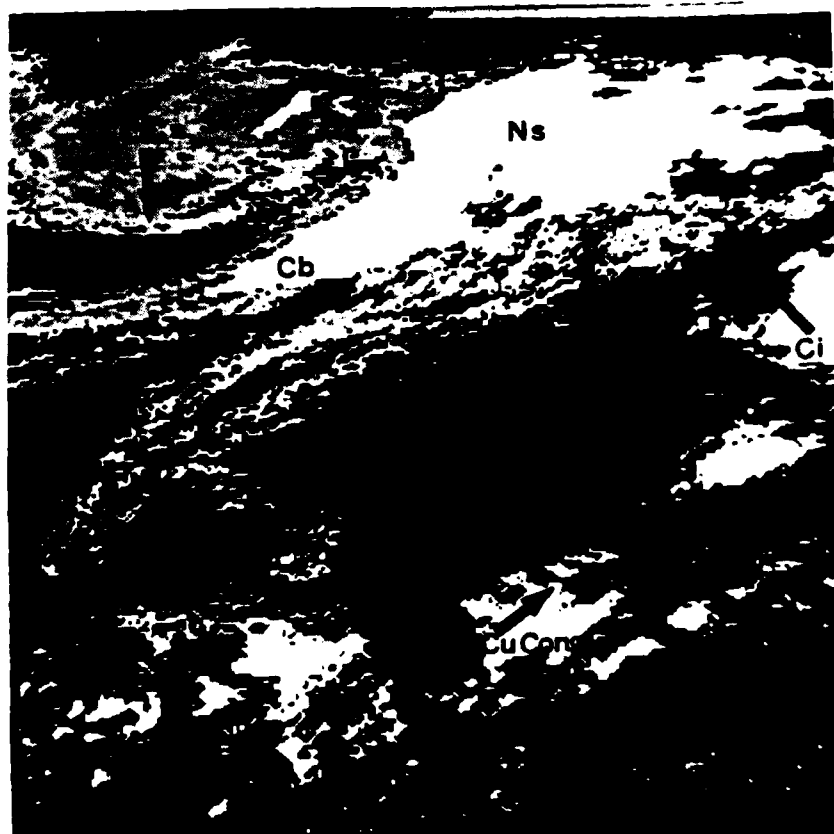


Fig. 10B. Same as Fig. 5B except for 11 AUG 83.

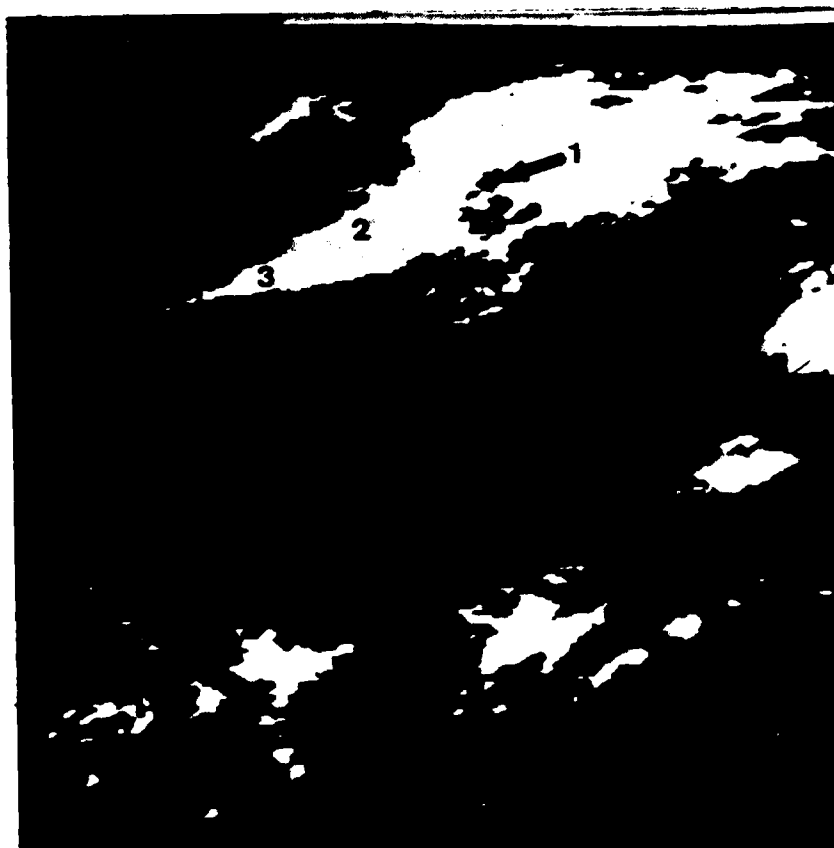


Fig. 10C. Same as Fig. 5C except for 11 AUG 83.

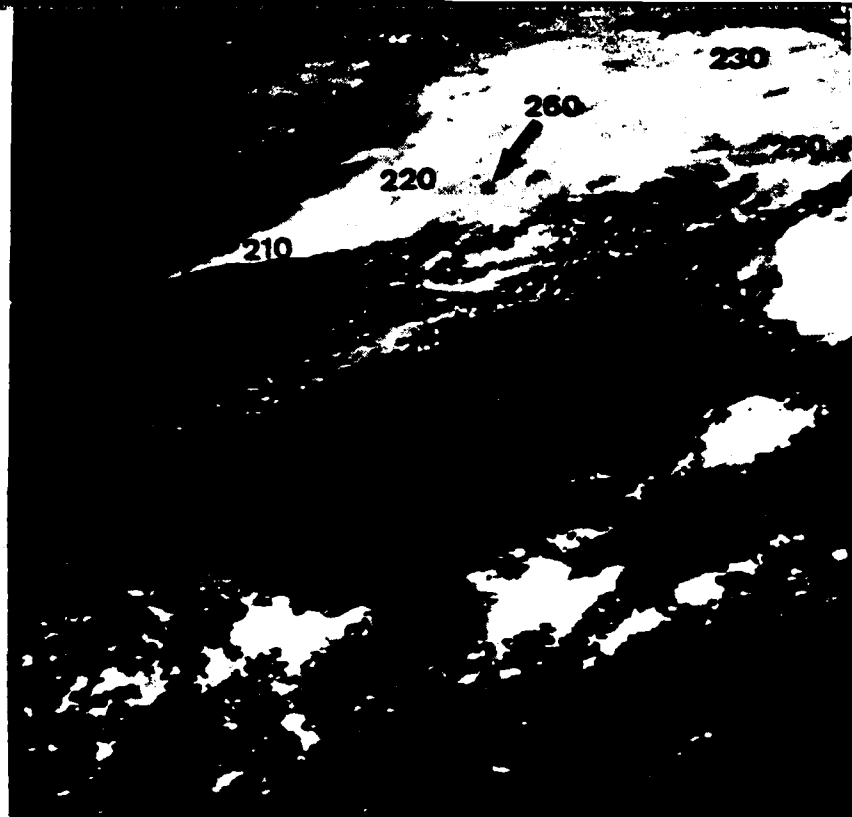


Fig. 10D. Same as Fig. 5D except for 11 AUG 83.

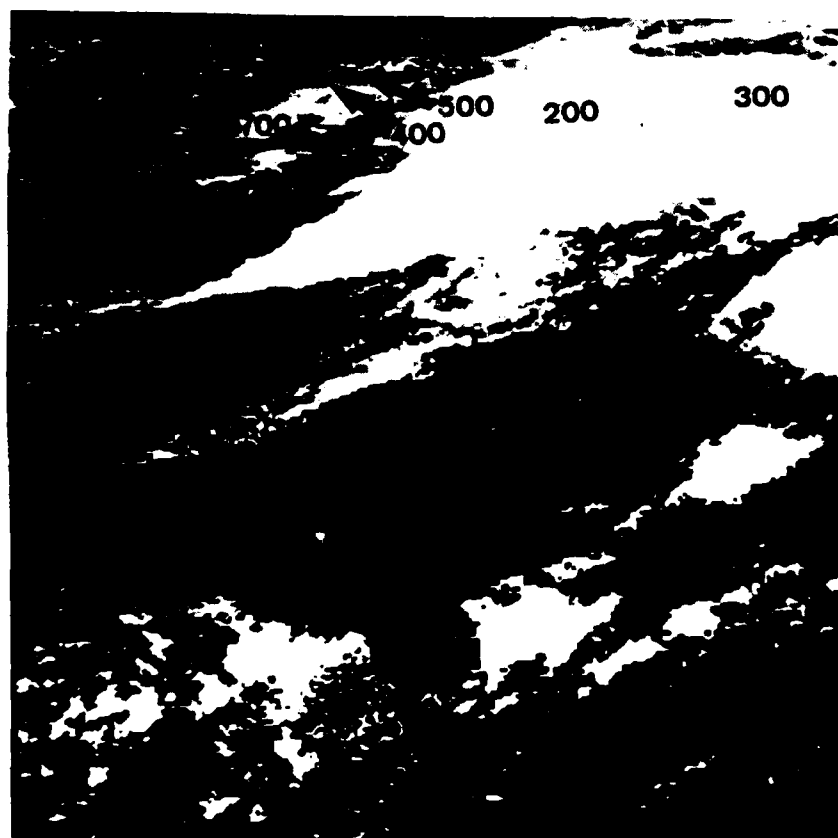
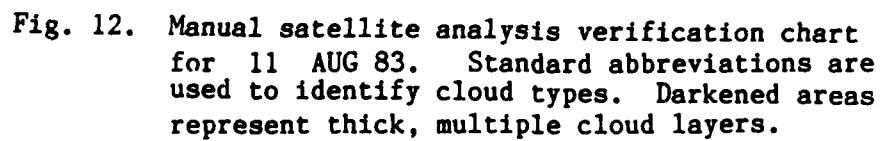


Fig. 10E. Same as Fig. 5E except for 11 AUG 83.



71



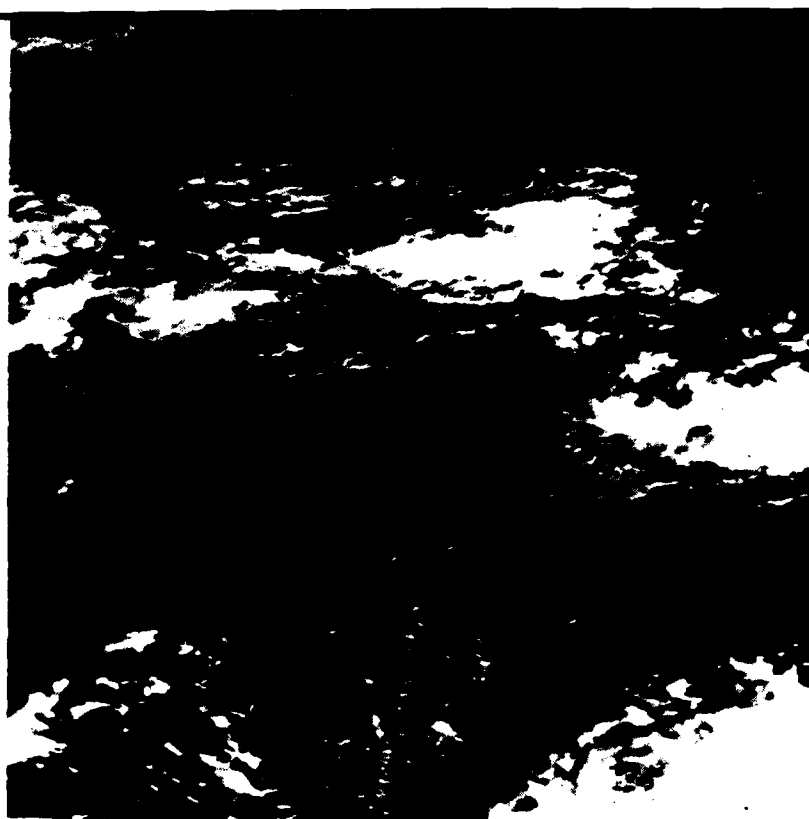


Fig. 13. GOES VIS imagery for 23 AUG 83.



Fig. 14. GOES IR imagery for 23 AUG 83.



Fig. 15A. Same as Fig. 5A except for 23 AUG 83.



Fig. 15B. Same as Fig. 5B except for 23 AUG 83.



Fig. 15C. Same as Fig. 5C except for 23 AUG 83.



Fig. 15D. Same as Fig. 5D except for 23 AUG 83.

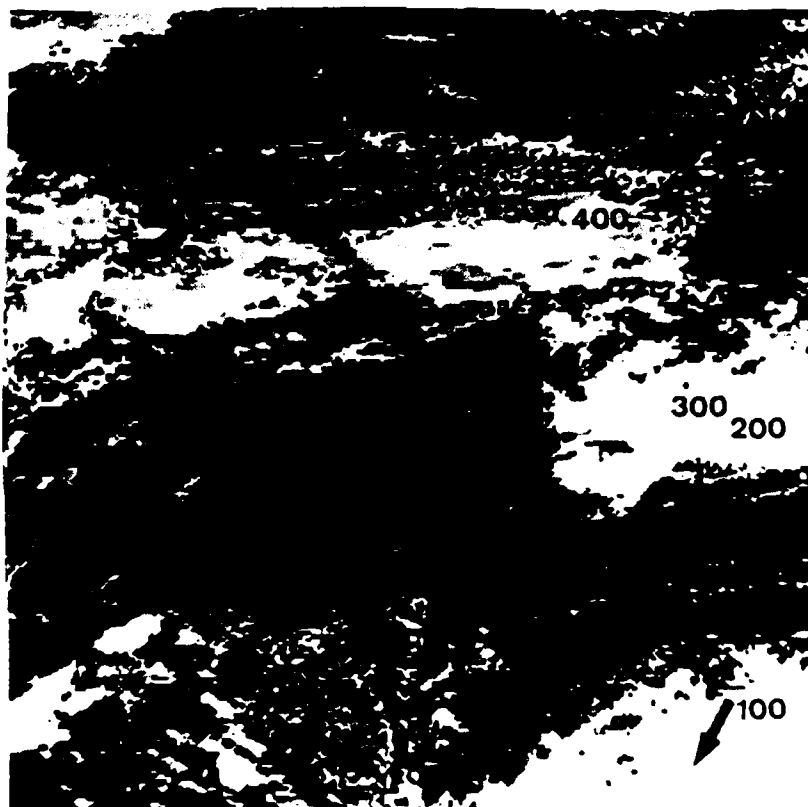
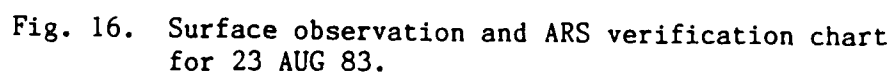


Fig. 15E. Same as Fig. 5E except for 23 AUG 83.





23 AUG 83

Fig. 17. Manual satellite analysis verification chart for 23 AUG 83. Standard abbreviations are used to identify cloud types. The abbreviations MLMC and ML Cld are used for multi-layered middle cloud and multi-layered cloud, respectively. Darkened areas represent thick, multiple cloud layers.

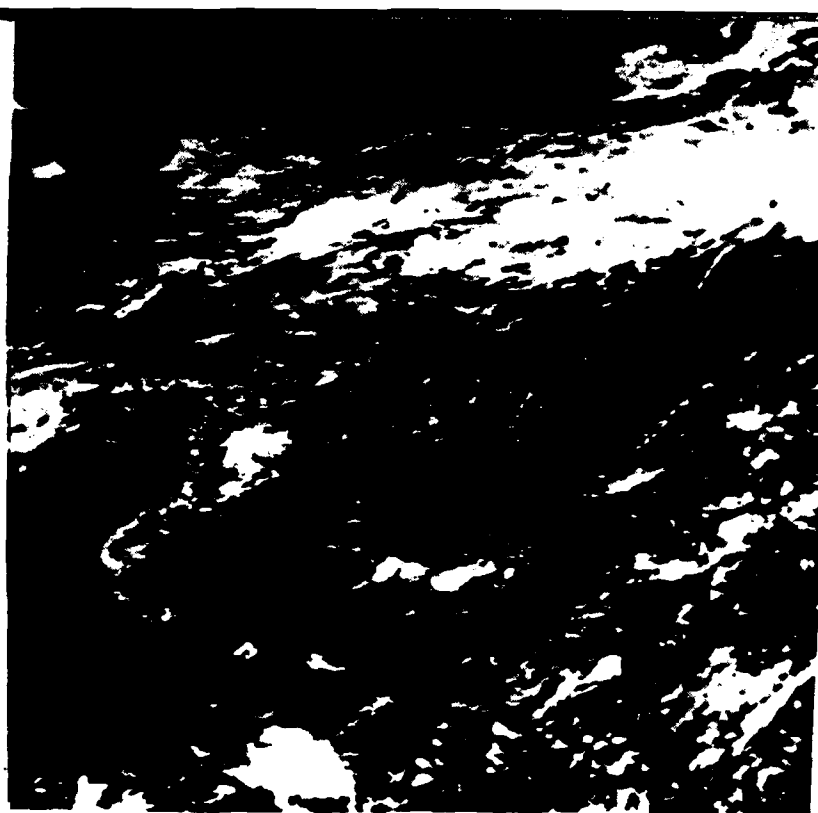


Fig. 18. GOES VIS imagery for 31 AUG 83.

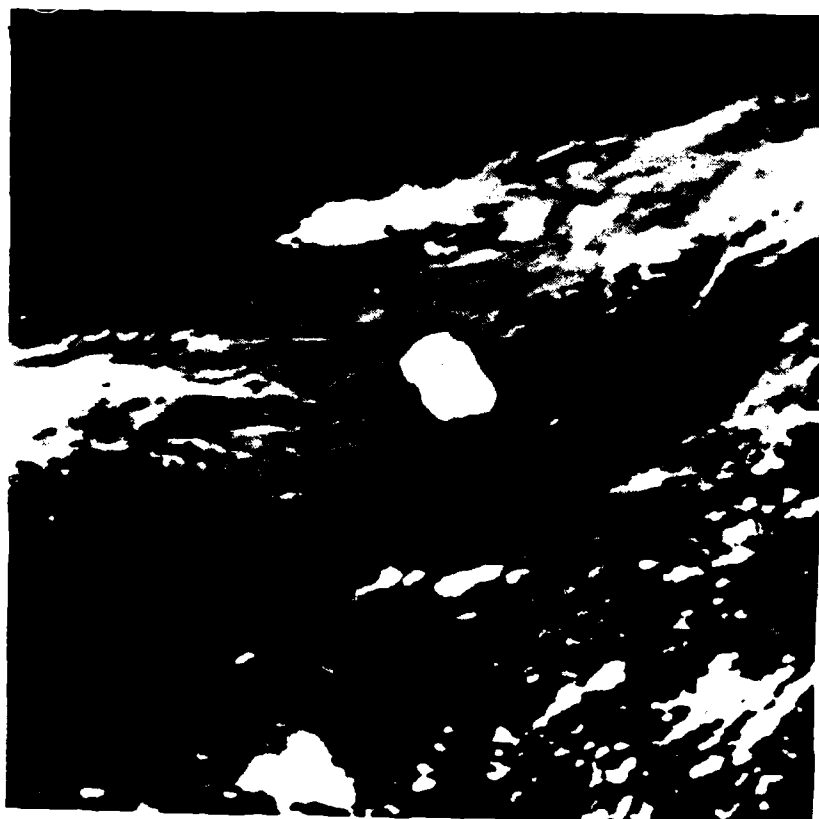


Fig. 19. GOES IR imagery for 31 AUG 83.

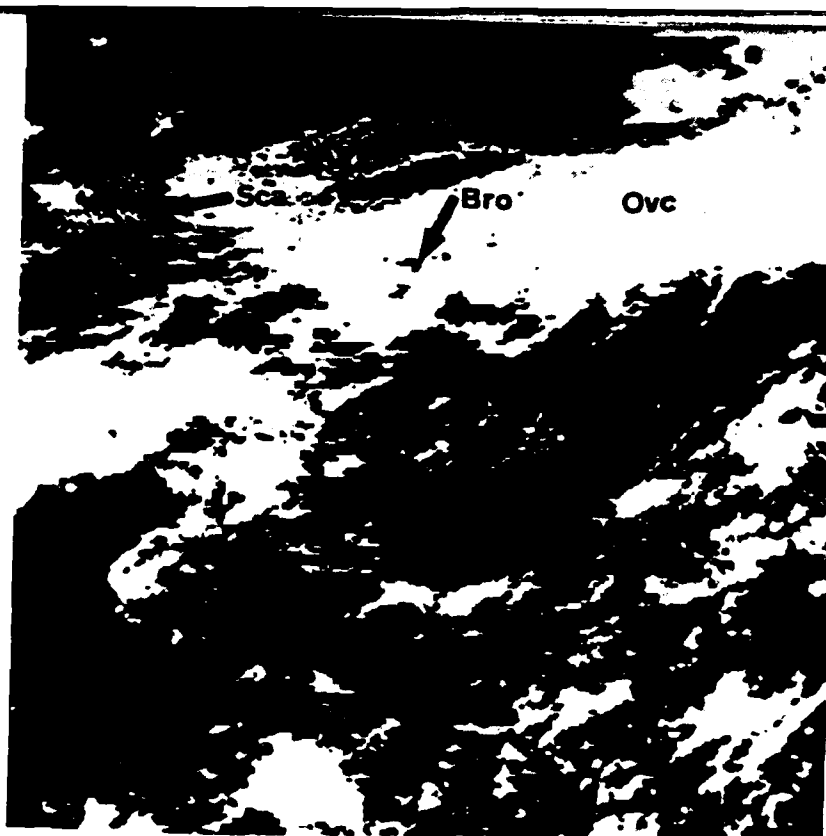


Fig. 20A. Same as Fig. 5A except for 31 AUG 83.

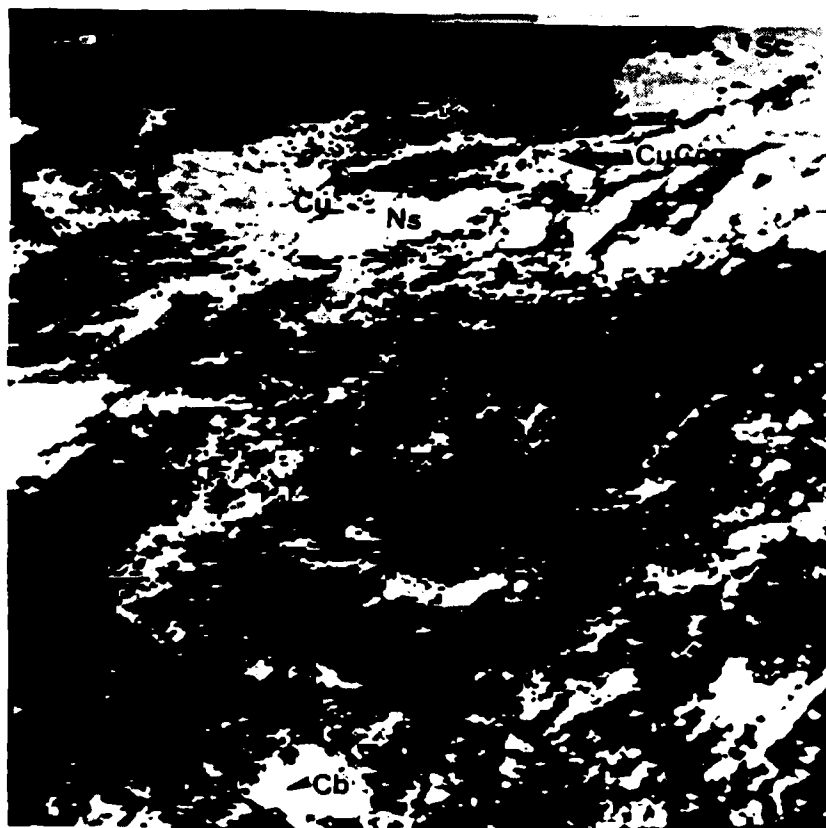


Fig. 20B. Same as Fig. 5B except for 31 AUG 83.



Fig. 20C. Same as Fig. 5C except for 31 AUG 83.

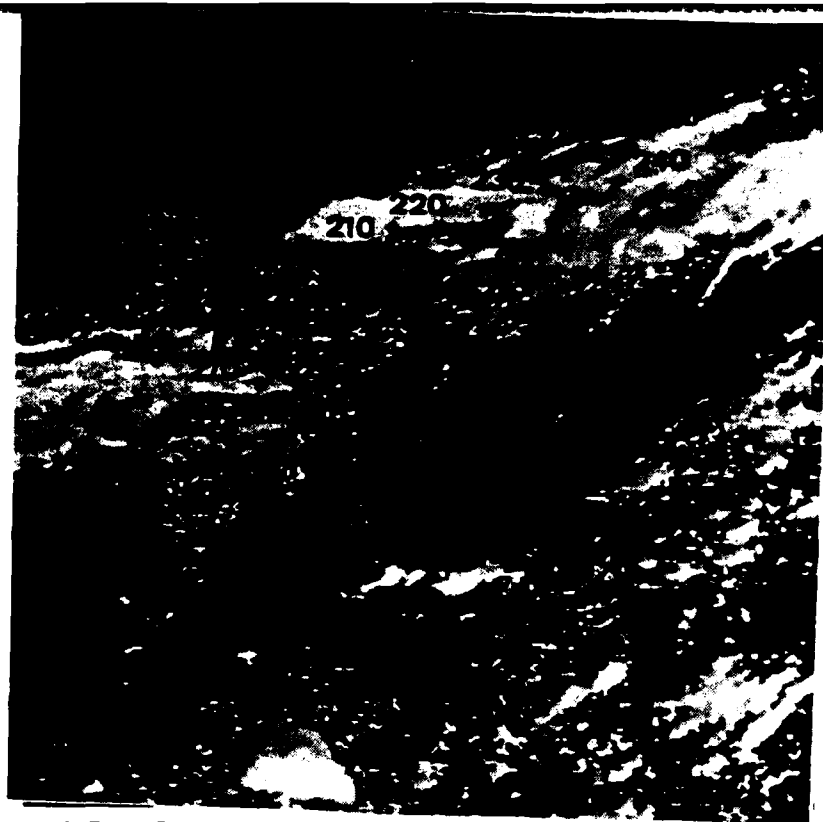


Fig. 20D. Same as Fig. 5D except for 31 AUG 83.

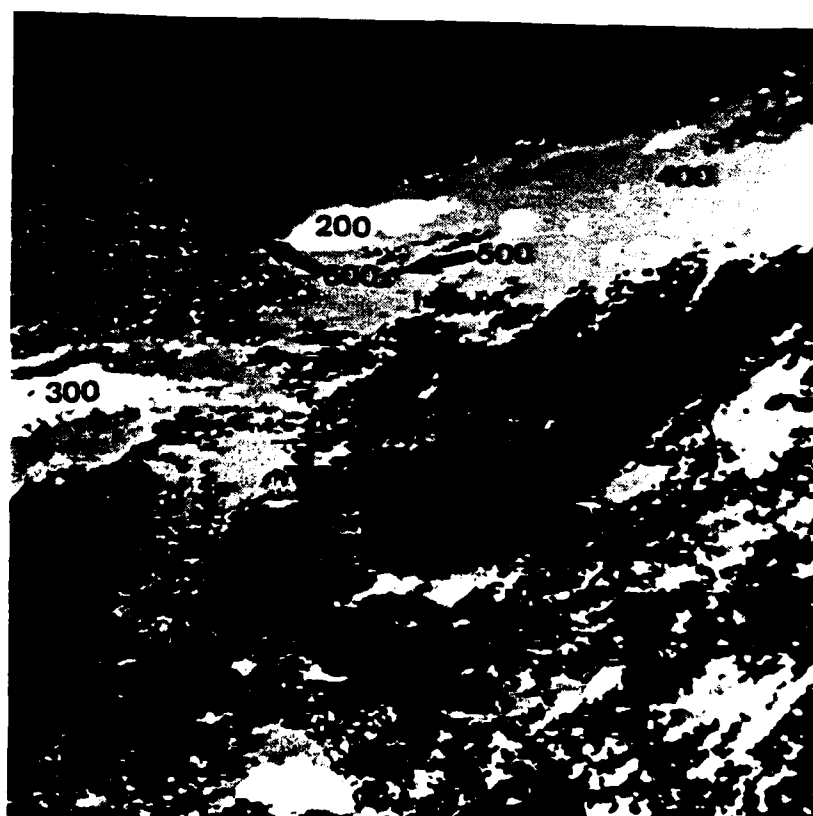


Fig. 20E. Same as Fig. 5E except for 31 AUG 83.

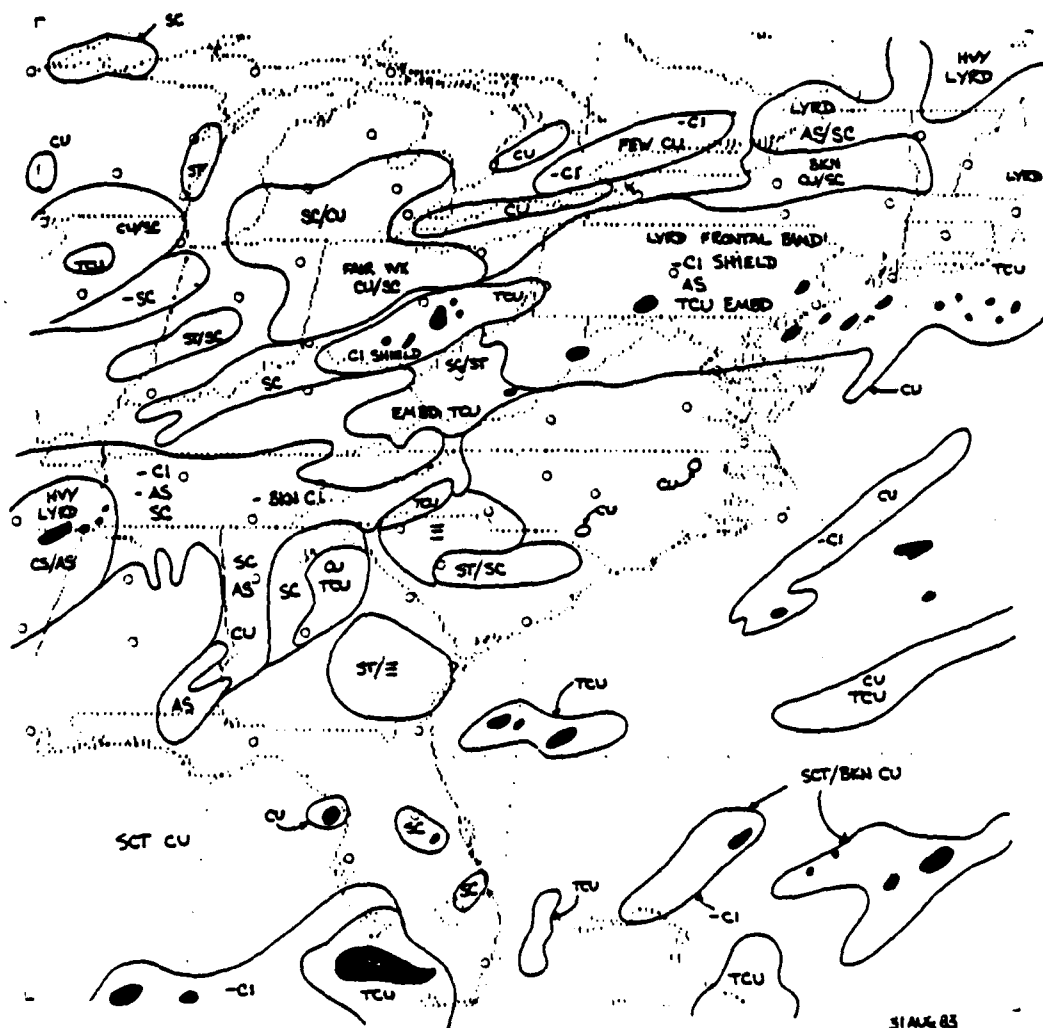


Fig. 22. Manual satellite analysis verification chart for 31 AUG 83. Standard abbreviations are used to identify cloud types. Darkened areas represent thick, multiple cloud layers.

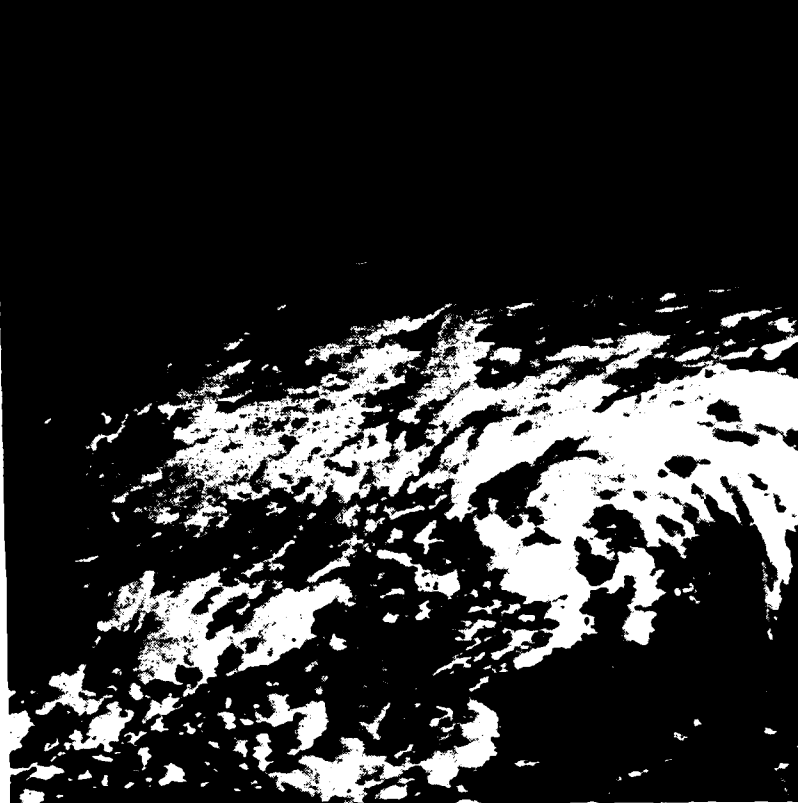


Fig. 23. GOES VIS imagery for 02 SEP 83.

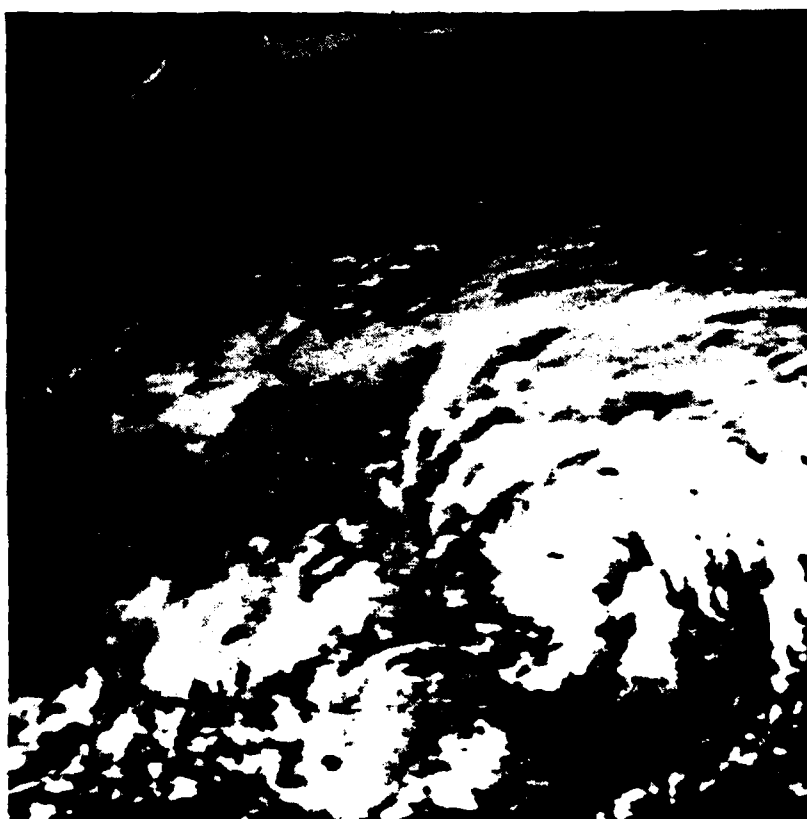


Fig. 24. GOES IR imagery for 02 SEP 83.

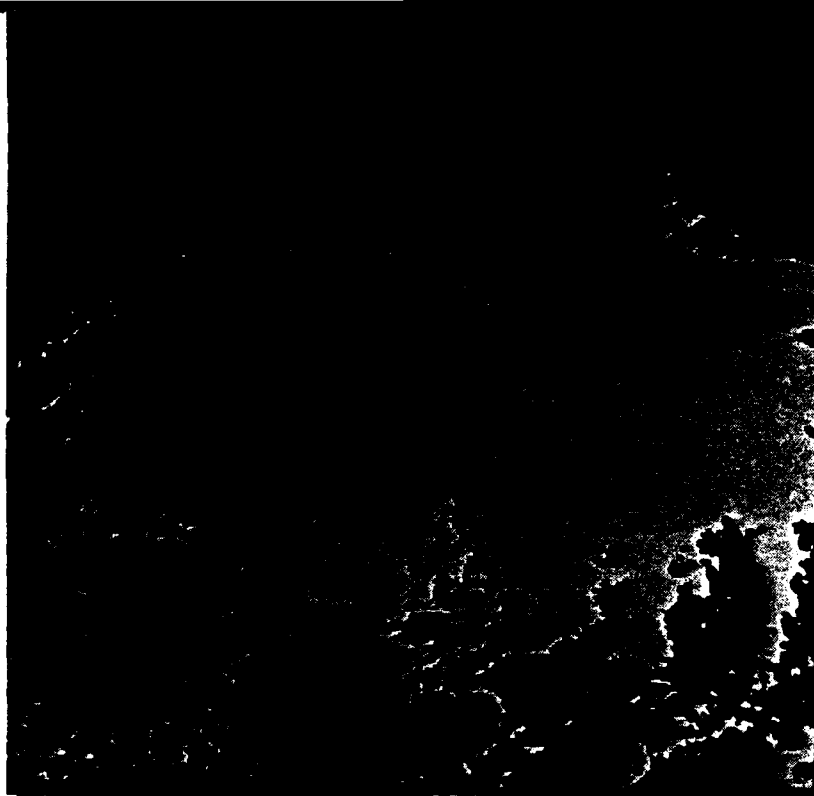


Fig. 25A. Same as Fig. 5A except for 02 SEP 83.



Fig. 25B. Same as Fig. 5B except for 02 SEP 83.

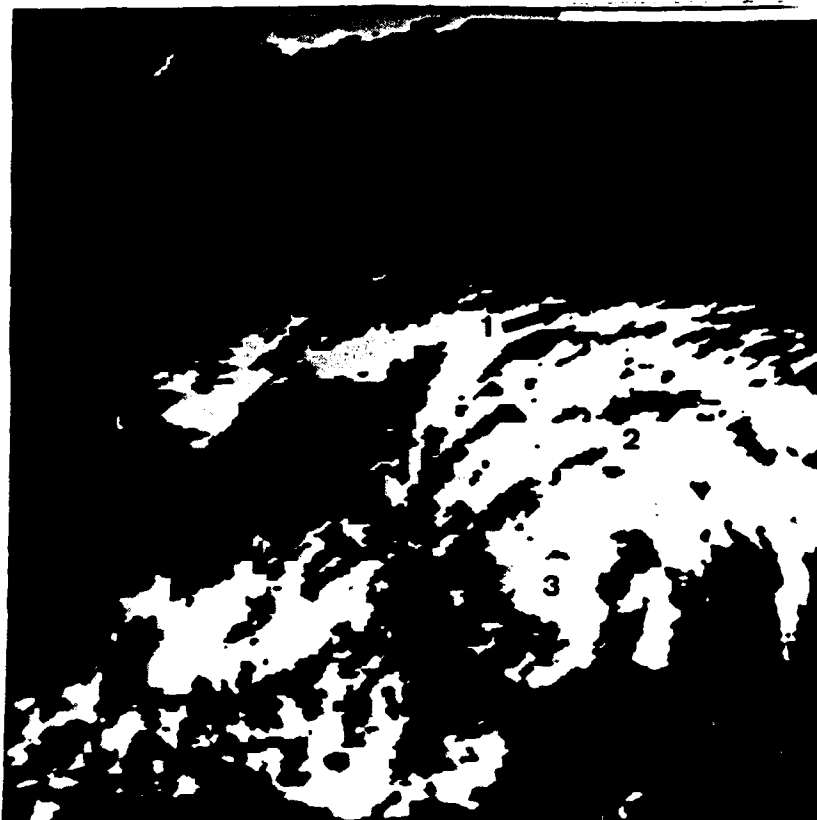


Fig. 25C. Same as Fig. 5C except for 02 SEP 83.



Fig. 25D. Same as Fig. 5D except for 02 SEP 83.

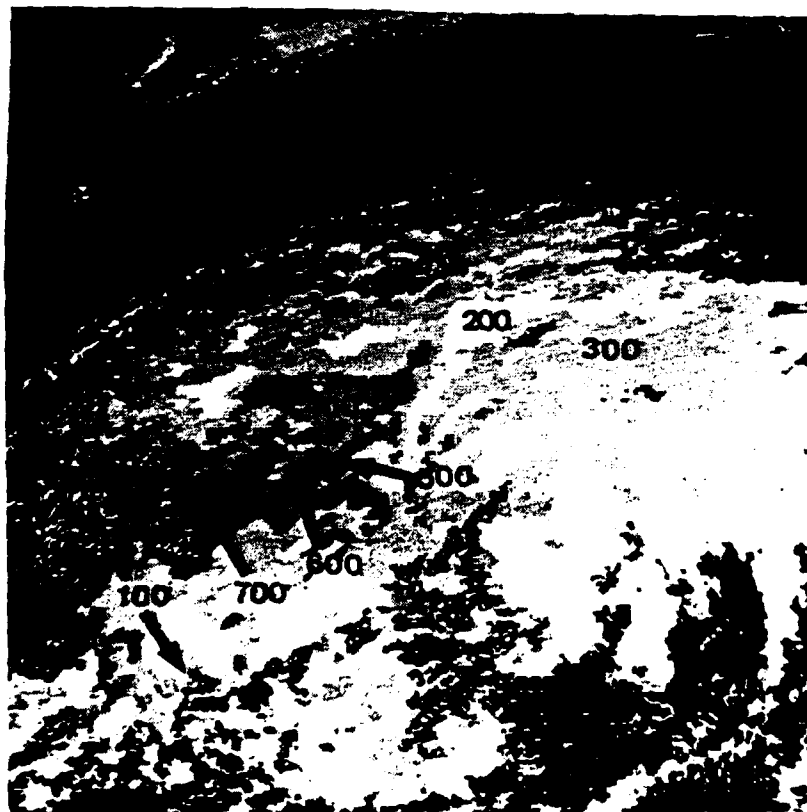
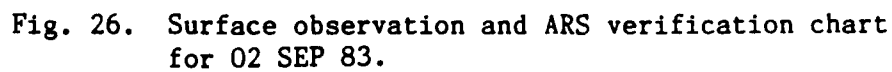


Fig. 25E. Same as Fig. 5E except for 02 SEP 83.



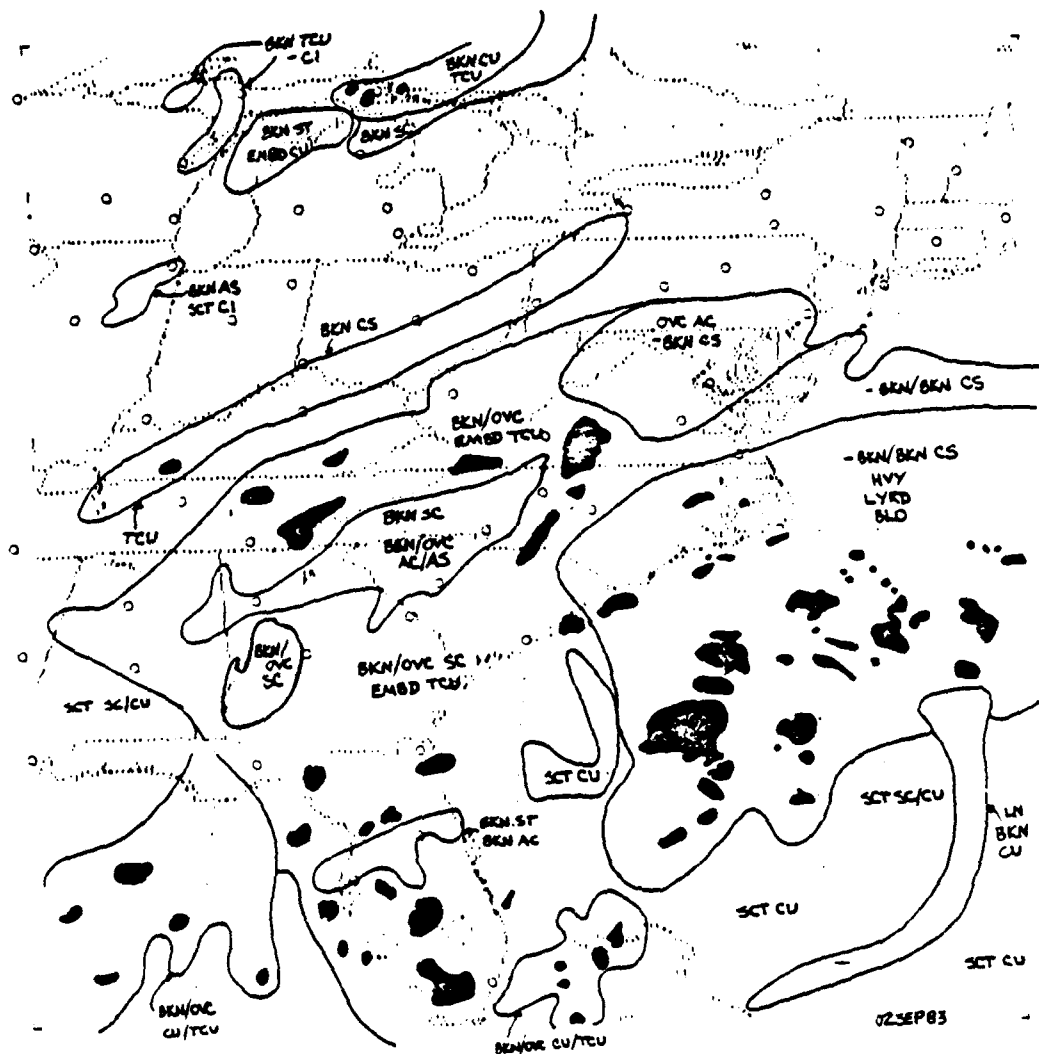


Fig. 27. Manual satellite analysis verification chart for 02 SEP 83. Standard abbreviations are used to identify cloud types. Darkened areas represent thick, multiple cloud layers.

INITIAL DISTRIBUTION LIST

	No. of Copies
1. Defense Technical Information Center Cameron Station Alexandria, Virginia 22314	2
2. Library, Code 0142 Naval Postgraduate School Monterey, California 93943	2
3. Department of Meteorology Library Code 63, Naval Postgraduate School Monterey, California 93943	1
4. Ms. Laura Spray, Code 63Sp Naval Postgraduate School Monterey, California 93943	2
5. Prof. C. H. Wash, Code 63Wx Naval Postgraduate School Monterey, California 93943	30
6. Commander Naval Oceanography Command NSTL Station Bay St. Louis, Missouri 39529	1
7. Commanding Officer Naval Oceanographic Center NSTL Station Bay St. Louis, Missouri 39529	1
8. Commanding Officer Naval Ocean Research and Development Activity NSTL Station Bay St. Louis, Missouri 39529	1
9. Commanding Officer Naval Environmental Prediction Research Facility Monterey, California 93943	1
10. Chairman, Oceanography Department U.S. Naval Academy Annapolis, Maryland 21402	1
11. Office of Naval Research (Code 480) Naval Ocean Research and Development Activity NSTL Station Bay St. Louis, Missouri 39529	1
12. Prof. R.J. Renard, Code 63Rd Naval Postgraduate School Monterey, California 93943	1